AMERICAN UNIVERSITY OF BEIRUT

EN-MASSE DISTALIZATION OF THE MAXILLARY DENTITION STUDIED WITH FINITE ELEMENT ANALYSIS

by
FIRAS NASSER NASSAR

A thesis
submitted in partial fulfillment of the requirements
for the degree of Master of Science
to the Department of Dentofacial Medicine
of the Faculty of Medicine
at the American University of Beirut

Beirut, Lebanon
March 2025

AMERICAN UNIVERSITY OF BEIRUT

EN-MASSE DISTALIZATION OF THE MAXILLARY DENTITION STUDIED WITH FINITE ELEMENT ANALYSIS

by

FIRAS NASSER NASSAR

Approved by:

Dr. Kinan Zeno, Assistant Professor of Clinical Specialty Department of Dentofacial Medicine	Advisor
Dr. Joseph Ghafari, Professor Department of Dentofacial Medicine	Co-Advisor
Dr. Samir Mustapha, Associate Professor Department of Mechanical Engineering	Member of Committee
Dr. Makram Ammoury, Adjunct Clinical Instructor Department of Dentofacial Medicine	Member of Committee

Date of thesis defense: March 19, 2025

ACKNOWLEDGEMENTS

First and foremost, I extend my deepest appreciation to the pillar of not just our department but of orthodontics in the region, Joseph Ghafari, our esteemed chairperson, who holds everything together. Without you, none of this would be possible. Your leadership, wisdom, and relentless dedication have been the foundation of our success. I am eternally grateful for the life-changing opportunity you have given me.

To Dr. Ramzi Haddad, the biomechanics guru, whose passion and expertise have inspired me to think beyond the obvious. More than just theory, you've made biomechanics one of the aspects I enjoy most in clinical practice.

To Dr. Anthony Macari, you never let me settle for anything less than excellence—your push, your high standards, and your unwavering belief in my potential have driven me to be my best.

A special thanks goes to Drs. Kinan Zeno and Makram Ammoury, both of whom have been more than just mentors—they have been like brothers. Your role in my thesis was nothing short of crucial, and your generosity in sharing knowledge made all the difference, making you the ultimate orthodontic dynamic duo.

I am also deeply grateful to Dr. Samir Mustapha, whose expertise in Finite Element Analysis made all the difference. Your patience, guidance, and ability to simplify what I initially thought would be an unsolvable puzzle made it possible.

I would also like to extend my sincere appreciation to Dr. Antoine Hanna for his dedicated efforts and valuable contributions to the statistical analysis.

To my incredible friends and colleagues, past and present, who have made this journey so much more meaningful—your friendship has been my strength. To my classmates, Marc and Cesar, the ones who truly understood every triumph and struggle—Marc, your presence made every challenge easier, and Cesar, my roommate, my partner in crime, my brother for the past four years, our shared experiences will forever be some of the most cherished memories of my life. And then came Christian—our roommate in our senior year, who turned it into a legendary mix of energy, making it truly unforgettable.

To my beloved family, who have supported me unconditionally, whose love and encouragement have been my rock—I owe everything to you. Your belief in me has carried me through the hardest moments and made the victories even sweeter.

And finally, to my lovely fiancée, Siham, the one who has been my greatest support, my anchor, and my motivation throughout this entire residency. Your unwavering presence in my life, your patience, and your boundless love have made this journey possible. Thank you for being my safe haven, and for sharing in every moment of joy and triumph.

This achievement is not mine alone—it belongs to all of you. From the bottom of my heart, thank you.

ABSTRACT

OF THE THESIS OF

Firas Nasser Nassar for Master of Science
Major: Orthodontics

Title: En-Masse Distalization of the Maxillary Dentition Studied with Finite Element Analysis

Introduction: En-masse distalization of the maxillary dentition is a widely used technique in orthodontics for correcting Class II malocclusions. While various force magnitudes and directions are employed in clinical practice, their precise effects on stress distribution and displacement remain inadequately understood. Also, variations in force magnitude and distalization modality may significantly affect biomechanical outcomes. Finite element analysis (FEA) offers a powerful tool for simulating orthodontic forces and assessing biomechanical responses in a controlled setting.

Aims: To compare stress distribution in the PDL and displacement patterns of the studied maxillary dentition under 200 g and 300 g of force.
To evaluate the effects of buccal, palatal, and bucco-palatal distalization modalities on tooth movement.
To determine which of the studied dentition experiences the highest stress levels and greatest displacement in response to distalization forces.
To analyze the influence of cortical bone thickness and stiffness on resistance to tooth movement.

Materials and methods: A three-dimensional finite element model of the maxillary dentition was generated using data from cone-beam computed tomography. Variations in cortical bone thickness and stiffness were incorporated across 13 and 11 models, respectively. Three distalization modalities were analyzed: buccal force (from a buccal miniscrew), palatal force (from a palatal miniscrew), and combined bucco-palatal force. Two force magnitudes (200 g and 300 g) were applied to the maxillary canines, with stress evaluated at the periodontal ligament (PDL) and displacement assessed at the occlusal surfaces of crowns and apices of roots. The models were meshed and analyzed using ABAQUS software, and statistical comparisons were made between different force magnitudes, distalization modalities, and cortical bone variations.

Results: Force magnitude and application method significantly influenced stress distribution and tooth displacement. The 300 g force led to greater displacement than the 200 g force but also generated higher stress levels on the PDL. Buccal force application resulted in the greatest displacement among the studied dentition, while palatal force produced tipping of the canine crown in the opposite direction. The combined bucco-palatal force modality facilitated a more balanced distalization. Moreover, the central incisor underwent the greatest displacement compared to all other

teeth. In contrast, the molar exhibited the least displacement across all distalization modalities. The canine experienced the highest stress levels, followed by the lateral incisor. Additionally, cortical bone stiffness affected tooth movement; models with stiffer cortical bone exhibited lower displacement and higher stress concentrations, indicating greater resistance to distalization.

Conclusion:

- The canine experienced the highest stress, followed by the lateral and central incisors. The central incisor showed lower stress, and higher displacement compared to the others. The lateral incisor and canine had higher stress but less displacement, suggesting greater resistance to movement, influenced by anatomical factors like tooth position, root length, and bone structure.
- Anchorage modality significantly affects stress distribution and displacement. Buccal anchorage caused the highest displacement, followed by bucco-palatal and palatal modalities. The palatal modality led to canine tipping, requiring clinical control or compensation.
- Applying 300g of force resulted in greater displacement of maxillary teeth and higher stress recorded in the periodontal ligament.
- The model's strength lies in incorporating individual variations in mechanical properties, showing that stiffness has a greater impact on resistance to displacement than thickness.
- Future studies should investigate the long-term effects of stress distribution on bone remodeling using CT scans of multiple individuals and time-dependent simulations for continuous tooth movement. Clinical validation via patient-specific finite element modeling would enhance the findings' applicability.

TABLE OF CONTENTS

ACKNOWLEDGEMENTS 1

ABSTRACT 2

TABLE OF CONTENTS 4

ILLUSTRATIONS 8

TABLES 11

INTRODUCTION 13

LITERATURE REVIEW 16

2.1 Treatment of Class II Malocclusion..... 16

2.1.1. Introduction to Class II Malocclusion 16

2.1.2 Definition and Classification 16

2.1.3. Class II Orthopedic Appliances 18

2.1.4 Class II Elastics..... 21

2.1.5 Temporary Anchorage Devices (TADs)..... 22

2.1.6 Extraction of Maxillary First Premolars 28

2.2 Maxillary Anatomy and Biomechanics of Tooth Movement 29

2.2.1 Maxillary Bones and Teeth..... 29

30

2.2.2 Biomechanics of Tooth Movement..... 30

2.3 Finite Element Analysis in Dentistry..... 31

2.3.1 Introduction to Finite Element Analysis..... 31

2.3.2 Basics of Finite Element Modeling 33

2.3.3 Applications of Finite Element Modeling in Dentistry 35
2.3.4 Types of 3D Imaging Technologies 36
2.3.5 Applications in Dental Research and Practice 37
2.3.6 FEA in Orthodontics 39

2.4 En-Masse Distalization Techniques 41

2.4.1 Overview 41
2.4.2 Types of En-Masse Distalization Appliance 42
2.4.3 Force Magnitudes in En-Masse Distalization Studies 44

2.5 Significance 47

2.6 Specific Objectives 48

MATERIALS AND METHODS 49

3.1 Materials 49

3.2 Methods 50

3.2.1 Distalization Setup 50
53
3.2.2 Meshing 53
3.2.3 Finite Element Analysis 53
3.2.4 Material Properties 54
3.2.5 Boundary Conditions 55
3.2.6 Interactions 56
58
3.2.7 Load 58
3.2.8 Data Collection and Export 59

3.3 Statistical Analysis 63

RESULTS 64

4.1 Force Magnitude Of 200 Grams 64

4.1.1 Stiffness Variation 64
4.1.2 Thickness Variation 66

4.2. Force Magnitude of 300 Grams 69

4.2.1 Stiffness Variation 69
4.2.2Thickness Variation 71

4.3 Comparison of Stress and Displacement Under Variation in Force Magnitude (200 Vs 300g) 74

4.3.1 Stiffness Variation 74
4.3.2 Thickness Variation 75

4.4 Comparison of Stress and Displacement in Relation to Treatment Modalities 77

4.4.1 Stiffness Variation 77
4.4.2 Thickness Variation 79

DISCUSSION 82

5.1 Differential Response to Distal Forces on Teeth 82

5.1.1 Stress Analysis 82
5.1.2 Displacement Analysis 83
5.1.3 Displacement-To-Stress Ratios (D/S) 85

5.2 Significance of Force Direction 87

5.2.1 Comparison of Stress and Displacement Across BP And P As a Function Of B 87

5.3 Differential Gradient of Forces (200 Vs 300 G) On Stress and Displacement 88

5.4 Clinical Implications 88

5.5 Research Considerations 89

5.5.1 Strengths 89
5.5.2 Limitations 91

CONCLUSION 95

REFERENCES 97

ILLUSTRATIONS

1. Figure 2.1: Intraoral and extraoral representation of a patient with Class II malocclusion characterized by a distocclusion of the dentition and retrognathic position of the mandible 17
2. Figure 2.2: Class II malocclusion as defined by Angle; mesio-buccal cusp of the maxillary first molar occludes mesial to the mesio-buccal groove of the mandibular first molar, and the mesial incline of the maxillary canine is mesial to the distal slope of the mandibular canine 17
3. Figure 2.3: Extraoral representation of a patient wearing a low-pull (cervical) headgear. 20
4. Figure 2.4: Inter-arch elastics used to correct Class II malocclusions. Typical Class II elastics are usually given from the maxillary canines to the mandibular molars..... 22
5. Figure 2.5: TAD used as direct anchorage to distalize the maxillary anterior teeth en-masse into an extraction space 22
6. Figure 2.6: Modified C-Palatal Plate appliance utilizing 3 palatal TADs 23
7. Figure 2.7: Buccally positioned used to distalize en masse the maxillary anterior teeth. A: power chain directly to the maxillary canine. B: power chain to power arm 25
8. Figure 2.8: TAD supported Forsus fatigue-resistant device used to treat Class II malocclusion 25
9. Figure 2.9: Pendulum appliance supported by anteriorly positioned palatal miniscrews. A: before activation, B: 5 months after treatment with molars moved distally and spacing apparent between the premolars 27
10. Figure 2.10: TAD supported distal jet appliance 28
11. Figure 2.11: Alveolar process on the labial/buccal portion of the maxilla 30
12. Figure 2.12: Palatine cortical bone at the level of the palatine vault, and trabecular bone which can be seen around the dentition inside the dental sockets 30
13. Figure 2.13: FEA of a model building prior to its construction displaying areas of critical stress for its design 33
14. Figure 2.14: FEA of the occlusal surface of molars after occlusion. This helps in identifying any high spots which can cause prematurity when biting. 36

15. Figure 2.15: A finite element analysis of a dental implant model being subjected to a force and the subsequent stress on the surface and surrounding bone are studied. 36

16. Figure 2.16: FEA of the maxillary dentition during orthodontic treatment..... 41

17. Figure 2.17 En-masse distalization of the entire maxillary dentition using buccally positioned 6 mm-long inter-radicular miniscrews 43

18. Figure 2.18: En-masse distaliztion of the entire maxillary dentition using palatally positioned miniscrews with: A: direct anchorage, and B: Indirect Anchorage 44

19. Figure 3.1: TAD level axial cut of the 12 models corresponding to 12 cadavers, based on the initial original model, with modified cortical bone thickness 50

20. Figure 3.2: TAD positioned on ScanIP™ (Simpleware, Synopsys) module along with its X, Y, & Z coordinates. Each coordinate has a position and orientation in space specified by (mm) and (degrees) respectively. 51

21. Figure 3.3: Palatal button sketched in Paint3D® software 52

22. Figure 3.4: 3D model of the final setup of the TADs and the palatal button 53

23. Figure 3.5: Boundary conditions: models constrained from translation and rotation at areas of attachments of the maxilla to adjacent bones: zygomatic, palatal, and sphenoid. A: superior view, and B: posterior view 55

24. Figure 3.6: Boundary conditions at the level of the maxillary dentition simulating the action of the brackets. A: frontal view showing the BC on the incisors. B: sagittal view showing the BC on the canines, premolars and molars 56

25. Figure 3.7: A: 3D Model in Abaqus software showing the interactions chosen between the maxillary dentition. B: the different interactions chosen mesial and distal to canine. Mesial to canine “Tie-constraint” interaction was chosen, however, distal to canine “surface-to-surface” interaction was chosen. 58

26. Figure 3.8: The 3 distalization modalities implemented in our study. **A**: buccal force delivered from a buccally positioned TAD. **B**: palatal force delivered from a palatally positioned TAD, and **C:** bucco-palatal force delivered from both buccally and palatally positioned TADs. 59

27. Figure 3.9: Selected elements on A: mesial, B: buccal, C: distal and D: palatal aspect of the maxillary canine, and similarly selected elements of E: mesial, F: buccal, G: distal, and H: palatal aspect of the maxillary first molar. These areas represent areas where stresses are to be measured and quantified. 60

28. Figure 3.10: Nodes chosen on the incisal tips of the canines, lateral incisors and central incisors. These nodes represent areas where displacement will be measured. 61

29. Figure 3.11: Nodes chosen on the apices of the canines, lateral incisors and central incisors. 61

30. Figure 3.12: Nodes selected on the A: occlusal surface of the maxillary first molar at the centroid region, and B: on the palatal and mesio-buccal roots of the maxillary first molar 62

31. Figure 4.1: Graphic representation of data in Table. 4.6 70

32. Figure 4.2: Graphic representation of data in Table. 4.8 73

33. Figure 4.3: Graphic representation of data in Table. 4.13 under 200g of force.. 78

34. Figure 4.4: Graphic representation of data in Table. 4.13 under 300g of force.. 79

35. Figure 4.5: Graphic representation of data in Table. 4.14 in the 200g force group 80

36. Figure 4.6: Graphic representation of data in Table. 4.14 in the 300g force group 81

37. Figure 5.1: Stress and displacement at the level of each tooth with the B modality. The colored areas correspond to the different material properties defined by Peterson et al in the maxilla (Fig. 3.1). 85

38. Figure 5.2: Density (in mg/cm^3) and thickness (in mm) of cortical bone at the level of 3 zones: palatal to anterior teeth, palatal to premolars, and palatal to molars (Peterson et al, 2006) 86

39. Figure 5.3: The highest displacement ($x10^3$ mm) under thickness variation, found in the original CT model, subjected to variation in stiffness (high and lowest among all cadavers). Note the greater displacement under low stiffness 94

40. Figure 5.4: Lowest displacement ($x10^3$ mm) under thickness variation, found in one of the experimental models, subjected to variation in stiffness (high and lowest among all cadavers). Note the greater displacement under low stiffness. 94

TABLES

Table

3.1: coordinates (X, Y, Z) for the position of the miniscrew..... 52

3.2: Material properties of various anatomical components commonly used in orthodontic Finite Element Analysis studies (Field et al., 2009; Kojima et al., 2012; Lim et al., 2003)..... 54

3.3: Orthotropic material properties at the site of the palatal incisors area 55

4.1: Comparisons of mean von mises stress generated on the evaluated teeth among treatment modalities..... 65

4.2: Comparisons of mean displacement generated on the evaluated teeth among treatment modalities..... 66

4.3: Comparisons of mean von mises stress generated on the evaluated teeth..... 67

4.4: Comparisons of mean displacement generated on the evaluated teeth among treatment modalities..... 68

4.5: Comparisons of mean von mises stress generated on the evaluated teeth among treatment modalities..... 69

4.6: Comparisons of mean displacement generated on the evaluated teeth among treatment modalities..... 70

4.7: Comparisons of mean von mises stress generated on the evaluated teeth..... 72

4.8: Comparisons of mean displacement generated on the evaluated teeth among treatment modalities..... 73

4.9: Stress and displacement ratios of individual teeth across different modalities compared between force magnitudes (300 vs 200 grams)- under stiffness variation 75

4.10: Displacement to stress (D/S) ratios of individual teeth across different modalities in force magnitude groups (300 vs 200 grams)- under stiffness variation 75

4.11: Stress and displacement ratios of individual teeth across different modalities compared between force magnitudes (300 vs 200 grams)- under thickness variation 76

4.12: Displacement to stress (D/S) ratios of individual teeth across different modalities in force magnitude groups (300 vs 200 grams)- under stiffness variation 77

4.13: Stress and Displacement ($x10^{-4}$) comparison of measurements in BP and P modalities as percentages (%) of B modality under different forces (200 vs 300 grams) (Stiffness variation) 78

4.14: Stress and Displacement ($x10^{-4}$) comparison of measurements in BP and P modalities as percentages (%) of B modality under different forces (200 vs 300 grams) (Thickness variation) 80

CHAPTER 1

INTRODUCTION

Over time, several advances in orthodontics aimed to decrease treatment time, without compromising treatment outcome. Thus, the search for faster and more efficient treatment methods has been amplified in recent years. The basic aspect that guides the planning of orthodontics is to achieve ideal occlusion, while maintaining the integrity of the supporting structures of the teeth. To achieve this, continuous forces need to be delivered to the teeth to promote tooth movement without causing any damage to the periodontal ligament. The application of moments of force in orthodontics is crucial for controlling tooth movements, including rotations and tipping. By adjusting the moment-to-force ratio, orthodontists can control the type of tooth movement, such as tipping, translation, or root movement. (Burstone & Smith, 1984).

En-masse distalization is a common orthodontic practice for correcting Class II malocclusions and, more recently, to avoid premolar extractions. All these mechanics use forces of high magnitude with typical values of 200–300 grams, which are quite high compared to the normal orthodontic force (Choi et al, 2011). Normally, the orthodontic force value should reside between the ranges of 50 to 100 grams per tooth (Theodorou, 2019). However, dividing a value of 200-300 grams force on all of the maxillary dentition will result in a force magnitude per tooth ratio which is still considered light when compared to other orthodontic forces (Ammoury et al, 2019).

In dentistry, finite element modeling is successfully applied in modeling various dental tissues under physiological, pathological, or therapeutic conditions (Zeno & Ammoury et al, 2023). Some of its representative applications are analyses of stress in

hard dental tissues (Boțilă et al, 2024), distribution of forces in orthodontics (Consolaro et al, 2014), and loads on dental implants of different designs (Falcinelli, 2023), and the alveolar compact bone (Tian et al, 2022).

Finite element modeling has proved to be a reliable research tool within the field of orthodontic biomechanics (Ammoury et al, 2019). It is not only helpful in understanding a specific treatment mechanic but also essential when devising a novel appliance or when material modifications are part of experimental hypotheses. Due to ethical concerns and the inherent variation in human morphology and behavior, the finite element method provides an alternate approach to in vitro, ex vivo, or computerized simulation studies that utilize actual teeth or patients. However, there are some limitations that must be recognized when using finite element models in discrimination methodologies for in vitro studies without an underpinning of previous mechano-biological knowledge (Trivedi et al, 2014).

The analysis of stresses and displacements resulting from buccal and palatal forces on maxillary dentition and PDL through FE modeling has received much attention in the literature of orthodontics. Building on the study by Shinya et al. (2009), the importance of PDL in tooth movement is explained as well as how direct application of orthodontic forces may result in ischemia and subsequent processes of remodeling within the periodontal tissue (Shinya et al., 2009). Their study shows the first tooth movement is mostly for the PDL displacement followed by the rest of the periodontium in subsequent movements to provide an understanding of biomechanics of orthodontic interventions. On this basis, F. Uhlir, (2014) goes further in analyzing the biomechanical description of the PDL, taking into account the problems encountered when using empirical approaches for the quantification of stress and strain during orthodontic tooth

movement (Uhlir et al, 2017). Uhlir focuses on the FE models, and the ways they call for a broader representation of non-linear stress/strain issue of the PDL, with the help of varying modulus representations. This improvement in modeling methods is significant for predicting movement of the teeth (Uhlir et al, 2017). The stresses and displacements caused by buccal and palatal forces are assessed in the study of Singh et al. (2016) through the use of FE modeling (Singh et al., 2016). Their work gives a practical analysis on how the sizes of forces alter the maxillary dentition and PDL.

In the existing literature, numerous clinical and finite element analysis (FEA) studies have investigated en-masse distalization as a treatment modality (Schwertner et al, 2024), (Lee et al, 2018), (Kawamura et al, 2021). However, a significant limitation emerges from the variation in the force magnitudes employed across these studies. Each study has utilized distinct force levels, tailored to specific experimental setups or clinical protocols, making it challenging to draw consistent conclusions or establish standardized guidelines. Notably, there is a lack of studies directly comparing the effects of different force magnitudes in terms of their efficiency and biomechanical outcomes. Sujaritwanid et al., (2021) focuses on the biomechanical effects of the distalization of one rather than two maxillary molars using FEA. They conclude that in order to distalize en masse a higher force value is required, which results in substantial tipping as well as extrusion on the molars. (Sujaritwanid et al, 2021).

Collectively these related studies constitute a strong evidence base of articles which not only explain the biomechanics of orthodontic tooth movement but also highlight the importance of FEM as a valuable research instrument in the field of clinical orthodontics and the importance of determining the quantity of force used in distalization.

CHAPTER 2

LITERATURE REVIEW

2.1 Treatment of Class II Malocclusion

2.1.1. Introduction to Class II Malocclusion

The Class II malocclusion is a very common but complex malocclusion. Its treatment is one of the biggest challenges in orthodontics (Ghodasra et al, 2024). Traditionally, extraction of the four first premolars has been extensively used to correct Class II malocclusions. However, with the advances in understanding the etiology and diagnosis of malocclusions, the tendency is to use non-extraction therapy in many cases of Class II malocclusions. The etiology of malocclusion is often multifactorial, related mainly to genetic and environmental factors. In addition, other factors must be considered to establish a good orthodontic plan. All these make the diagnostic and treatment plan of Class II malocclusions an extremely important step for orthodontic patients (Ghodasra et al, 2024).

2.1.2 Definition and Classification

Malocclusion can be described as the false position of teeth in any three dimensions of space (Prasad et al., 2014). Class II malocclusions account for over one-third of all malocclusions observed globally and are more common in Caucasians than in other races. Accordingly, in general dentistry practice, class II malocclusion patients make up about one-third of patients needing orthodontic treatment. This form of malocclusion is caused by a variety of causes (Proffit et al, 1998). Still, most research

reports have linked it to mandibular deficiency (mandibular retrognathia is the leading cause, rather than maxillary prognathism) (Fig. 2.1) (Fig. 2.2).

Figure 2.1: Intraoral and extraoral representation of a patient with Class II malocclusion characterized by a distocclusion of the dentition and retrognathic position of the mandible

Figure 2.2: Class II malocclusion as defined by Angle; mesio-buccal cusp of the maxillary first molar occludes mesial to the mesio-buccal groove of the mandibular first molar, and the mesial incline of the maxillary canine is mesial to the distal slope of the mandibular canine

Not all cases of malocclusion require intervention. The treatment urgency or priority commonly estimated by the Index of Orthodontic Treatment Need (IOTN), the Dental Aesthetic Index (DAI) and others, ranges from “No, little” — “Essential. Such discrepancies in occlusion may lead to social embarrassment since patients would always be so conscious when it comes to the appearances of their dental and facial structures during these functions. Aesthetics for many forms is the primary reason that they present themselves for orthodontic treatment even disregarding the fact that they represent a proactive intervention that can enhance not only form and function of teeth and jaws as well as their general health and well-being (Enzo et al, 2020).

When a child transitions into mixed dentition, any malocclusion of their permanent teeth starts developing. In the attempt to diagnose malocclusion, the skeleton may be used as a reference. If so, large variances are generally accepted for the evaluation of the accuracy of dating and prediction of growth derived from the skeleton for an individual. Causes of malocclusion are involved in congenital disorders, growth anomalies, disease, aging or death of some dento-craniofacial units, and to a lesser extent with spontaneous remodeling (Alogaibi & al., 2021). Even Class I malocclusions can persist due to their non-adaptive nature, resulting in untreated dental discrepancies. Simple dental, endocranial, or post-cranial causes of malocclusions are the minority among etiologies (Buschang, 2014).

2.1.3. Class II Orthopedic Appliances

Orthopedic appliances, or in other words, growth modification appliances are orthodontic devices that aim in enhancing differential growth of the mandible. They are usually used during the growth spurt, where growth is at its peak to take advantage of the

mandibular growth and to enable the correction of the skeletal Class II (Alhasyimi et al, 2023). These devices are usually given during the late mixed dentition or the early permanent. The duration and their efficacy depend on the rate of the adolescent's growth changes in combination with other factors such as genetics (Gurgel et al., 2023). Class II malocclusions can be the result of either an abnormal anterior mandibular position, an excessive anterior maxillary position, or a combination of the two. It is complex in nature and often associated with numerous dental problems, including an increased overjet and overbite, mandibular retrusion with or without an adequate chin (symphysial) anatomy (Ghafari et al, 2024), and depending on the subcategory of the Class II malocclusion, could be associated with either proclined or retroclined maxillary incisors. Class II malocclusion has a clear genetic component and a close correlation to abnormal growth, which is often observed as decreased growth of the mandibular structure and/or increased maxillary growth. The longitudinal analysis of craniofacial growth from the mixed dentition period to maturity has been well documented (Arat et al, 2001). However, reasonable methods for predicting future craniofacial growth and, especially, different growth patterns, are still lacking. The question of when orthodontists should begin treatment for skeletal Class II malocclusions is a largely unresolved issue. Although many orthodontists recognize skeletal Class II malocclusions in early mixed dentition, few specialists agree when to treat patients at this developmental stage. Many orthodontists commonly treat growing Class II patients with orthopedic or orthodontic treatment to minimize future Class II problems, taking advantage of the potential for growth modification in children. According to Ghafari et al, treating patients with Class II malocclusions is considered most efficient when initiated at either the late mixed dentition or early permanent dentition (Ghafari et al, 1998). Adolescents with severe

skeletal Class II discrepancies that cannot be eliminated by orthopedic or orthodontic treatment alone can be effectively treated with a combination of orthodontics and orthognathic surgery at growth cessation (Rédua et al, 2020).

2.1.3.1 Headgear

The headgear originated from an extraoral headcap and a high-pull extraoral traction device. Both are used to restrict the forward movement of the maxilla and enhance forward growth of the mandible (Fig. 2.3). The effectiveness of the headgear using a force of 400-450 grams relies mainly on patient compliance (Larissa et al, 2022).

Figure 2.3: Extraoral representation of a patient wearing a low-pull (cervical) headgear.

2.1.3.2 Activator/Bionator

The Bionator was one of the first functional appliances to be introduced in the 1960s. The effects of the Bionator in Class II growing patients evidenced that the Bionator induced skeletal effects characterized by forward movement of the chin, increasing mandibular length, and changes in maxillomandibular sagittal relationship into a more

favorable skeletal Class I, in accordance with the reduction of maxillomandibular discrepancy. The Bionator is a mandibular propeller Class II corrector featuring a metallic wire that surrounds the upper first molar and premolars, allowing these teeth to disocclude from the antagonist teeth. In order for rapid and significant results to be accomplished, however, it is paramount that the patient's cooperation, along with the growth phase, be well understood, as the ideal conditions for orthopedic correction to be accomplished are met through the functional maturation of the stomatognathic system (Achmad & Sesioria, 2022).

2.1.4 Class II Elastics

Class II elastics, worn between the maxillary anterior teeth and mandibular posterior teeth, exert forces that cause opposite effects: distalization of the maxillary buccal segments and protrusion of the mandibular teeth (Fig. 2.4). However, mandibular teeth are more prone to protrusion due to their lower resistance. In addition to influencing transverse and anteroposterior dimensions, these elastics create vertical forces that can lead to the extrusion of mandibular molars and maxillary anterior teeth, resulting in a clockwise rotation of the occlusal plane. In adult patients, this vertical effect often causes an undesirable backward and downward rotation of the mandible, increasing gingival display. As a result, Class II elastics are generally not recommended as the primary approach for Class II correction. Instead, their use is typically limited to short periods (3 to 4 months) to assist with anchorage or finalize occlusal adjustments (Proffit et al, 2012).

Figure 2.4: Inter-arch elastics used to correct Class II malocclusions. Typical Class II elastics are usually given from the maxillary canines to the mandibular molars

2.1.5 Temporary Anchorage Devices (TADs)

Anchorage control and patient compliance were practically resolved with the advent of temporary anchorage devices (TAD), also known as orthodontic miniscrews, micro-implants, and mini-implants (Papadopoulos & Tarawneh, 2007) (Fig. 2.5).

Figure 2.5: TAD used as direct anchorage to distalize the maxillary anterior teeth en-masse into an extraction space

Creekmore and Eklund (1983) advocated the use of a metallic screw inserted in the alveolar bone that can withstand constant force of sufficient magnitude and duration to reposition an entire anterior maxillary dentition without becoming loose, painful, infected, or pathologic. These implants are widely used because of the incomplete osseointegration, a distinct advantage in orthodontic applications, allowing for effective

anchorage with relatively easy insertion and removal (Crismani, 2010). The introduction of TADs enabled the orthodontist to distalize en-masse the entire maxillary dentition without risk of anterior anchorage loss (Bechtold, 2013).

Palatal miniscrews used for distalization are gaining popularity (Fig. 2.6), but interradicular TADs remain the most frequently used because they are comparatively easier to place and remove and they cause fewer irritation to soft tissues as they are placed in the attached gingiva (Arcuri et al, 2007). More cortical bone exists mesial to the maxillary first molars (1.8 +/-0.6 mm) allowing more TAD stability. It has been postulated that an insertion angle from 20 to 60 degrees allow optimal cortical bone engagement. Deguchi et al. (2006) noted that contact between the miniscrew and cortical bone increased by 1.5 times when angulated by 30 degrees. Laursen et al (2012) showed an increase in cortical bone-to-implant contact by an average of 47% when angulating the TAD by 45 degrees.

Figure 2.6: Modified C-Palatal Plate appliance utilizing 3 palatal TADs

2.1.5.1 Buccal Positioned TADs

Transmucosal or buccally anchored TADs have become favorably accepted due to the rapid placement technique and the absence of mucosal breaches and potential

irritation of the overlying tissue (Fig. 2.7). These devices have increased treatment possibilities and provided new ways of treating complex problems. One advantage of buccally placed implants is that they provide a more natural direction of force delivery. In a systematic review of studies involving these devices, only one study carried out a surgical process, penetrating the mucosa almost entirely, and presented a mucosal recession due to the irritation that usually occurs during teeth movements to open space for implants. On the other hand, the other studies reported no augmentation of gingival recession during the orthodontic treatment period (Ciarlantini & Melsen, 2012). They can be removed, adapted, or replaced in different areas with minimal risk of gingival inflammation or overgrowth and can stimulate or reactivate bone (Truong et al., 2022).

As a disadvantage, we have the need for more space and surgical assistance to perform the procedure, which favors the surgical process and requires gum healing, but it is easy to replace them or use them in different locations during appointments, foretelling a notable advantage over the days or weeks of workload that are necessary to place the TADs during the orthodontic treatment period. The buccal surgically assisted rapid palatal expansion technique has been successfully planned to treat dentofacial discrepancies in orthodontic patients without the need for general anesthesia and, in addition, can stimulate the presence of new bone in the tooth extraction sites that in the future could be used for space retraction (Riachy et al, 2023).

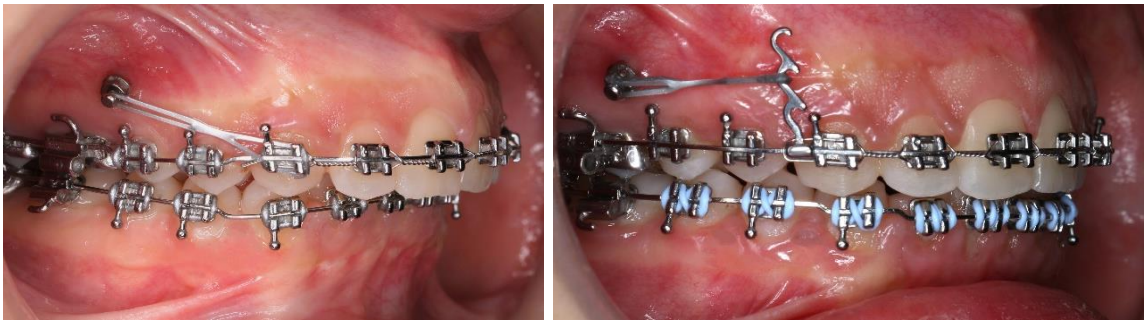

Figure 2.7: Buccally positioned used to distalize en masse the maxillary anterior teeth. A: power chain directly to the maxillary canine. B: power chain to power arm

Another appliance which utilized buccally positioned TADs is the Miniscrew-Anchored Forsus Appliance (Fig. 2.8). This appliance is a fixed functional appliance that, when combined with miniscrews, can assist in distalizing the molars while also addressing Class II malocclusion. It is effective for simultaneously correcting the sagittal relationship and distalizing the molars, making it a versatile treatment option. However, it may not be as effective as dedicated distalization appliances in achieving significant molar movement on its own (Rizwana et al, 2024) (Elkordy et al, 2019).

Figure 2.8: TAD supported Forsus fatigue-resistant device used to treat Class II malocclusion

2.1.5.2 Palatal Positioned TADs

Recently, palatally positioned TADs have become more popular and versatile in distalization of the maxillary dentition, albeit sectional or en-masse. Various palatal distalization modalities exist. Similar to the buccally positioned TADs, palatal TADs are mainly used for direct anchorage distalization. Other palatal distalization appliances exist such as i-Panda, modified C-palatal plate, miniscrew-supported distal jet appliance, etc. (Sujaritwanid et al, 2020)

A systematic review analyzed nine studies, including two RCTs and seven prospective cohort studies, to evaluate the effects of temporary skeletal anchorage devices (TSADS) placement on maxillary molar distalization. Palatal TSADs achieved the greatest distalization (4.07–4.17 mm) but caused significant distal tipping (11.17°), while infrazygomatic TSADs provided similar distalization (4.17 mm) with moderate tipping (3.99°). Buccal TSADs achieved the least distalization (2.75 mm) but minimized tipping (1.70°). All TSAD positions resulted in slight molar intrusion (0.60–0.69 mm), and treatment duration ranged from 5.3 months for palatal TSADs to 8.2 months for buccal placements. Palatal TSADs were associated with distobuccal rotation, while buccal placements caused mesio-buccal rotation, and second molar effects varied by placement site. Therefore, TSAD placement significantly influences outcomes, with palatal TSADs being effective for substantial distalization despite tipping risks, buccal placements offering precision with limited range, and infrazygomatic placements balancing both. However, there was variability in study designs and a lack of high-quality RCTs which underline the need for further research to determine optimal TSAD position (Bayome et al, 2021).

A systematic review by Mohamed et. al, provides a detailed comparison of several miniscrew-supported appliances used for maxillary molar distalization in Class II malocclusion (Mohamed & al, 2018). The key appliances discussed in the review are the following:

- Pendulum Appliances with Miniscrews:

  Modified pendulum appliances use miniscrews for skeletal anchorage, reducing the need for premolar or incisor anchorage (Fig. 2.9). These appliances effectively distalize the molars, with a significant range of movement, though some distal tipping of the molars may occur. A major advantage is that the patient's compliance is less critical, making it a reliable choice for many patients. However, the downside is the potential for tipping of the molars during movement (Sun et al, 2025).

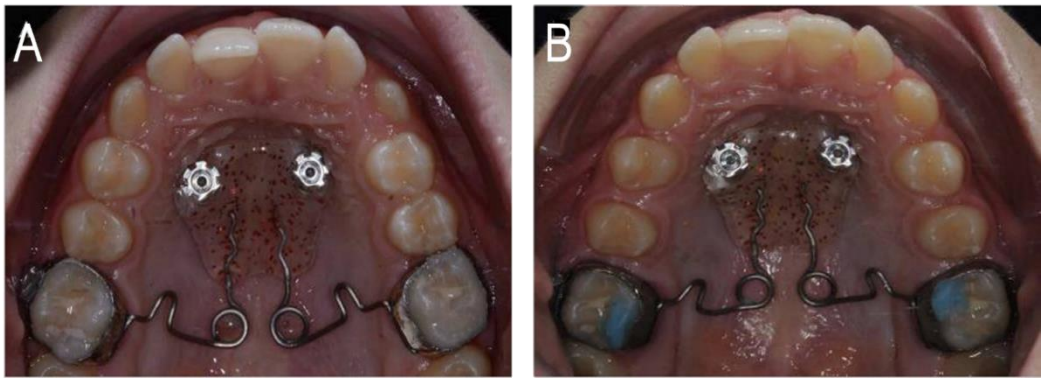

Figure 2.9: Pendulum appliance supported by anteriorly positioned palatal miniscrews. A: before activation, B: 5 months after treatment with molars moved distally and spacing apparent between the premolars

- Miniscrew-Supported Distal Jet:

The distal jet appliance, when combined with miniscrew support, minimizes mesial movement of the anterior teeth during molar distalization (Fig. 2.10). This appliance provides excellent control over molar movement, with minimal anchorage loss in the

premolars and incisors. It is more effective in controlling the angulation of the molars compared to the pendulum appliance, but it is less versatile for complex multi-tooth movements (Kinzinger et al, 2007).

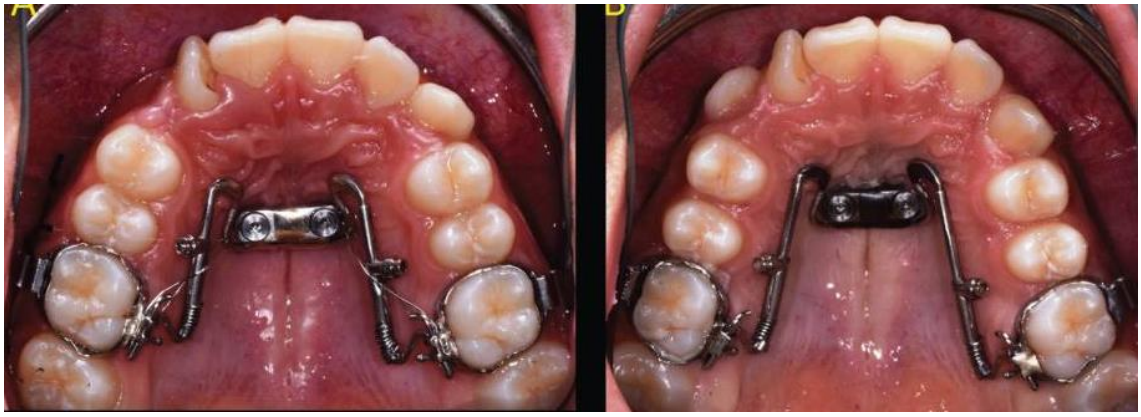

Figure 2.10: TAD supported distal jet appliance

2.1.6 Extraction of Maxillary First Premolars

The extraction of maxillary first premolars is an efficient alternative for the treatment of Angle Class II malocclusions, especially with the presence of mild or severe maxillary crowding, dental protrusion, or the discrepancy between the arch lengths. However, the treatment of these malocclusion criteria should be planned individually, considering the skeletal facial pattern, the position of maxillary and mandibular incisors, the facial analysis, and the esthetic facial and smile line characteristics of each patient.

Therefore, orthodontic therapies, whether they involve the extraction of the maxillary first premolars or not, are two factors that vary greatly from case to case, according to certain criteria. The orthodontic community has varied in its approaches regarding the treatment of maxillary first premolar extractions, particularly whether they can lead to excessive retrusion of the maxillary and mandibular incisors, which could

generate changes in the soft tissues (Tadic et al, 2007). Supporters of this treatment option argue that, when planned adequately, the results are reliable, stable, and the smile is harmonious; that is, all the esthetic goals are reached.

However, long-term observational studies on extracted cases and non-extraction cases have suggested that there would be no significant differences between the changes in facial profile in both types of treatment (Stephens et al, 2005). Quite the contrary, it does not seem that the profile was significantly altered when only the retraction of the maxillary incisors occurred (Stalpers & al, 2007).

2.2 Maxillary Anatomy and Biomechanics of Tooth Movement

2.2.1 Maxillary Bones and Teeth

The maxillary dentition is attached on two sides of the jaws by the maxilla bone itself, which surrounds the teeth above the alveolar process, providing structural support and stability (Figs. 2.11 & 2.12). This characteristic of the maxillary bone makes it largely dependent on the integrity of its basal bone. (Roesch et al, 2023).

Early studies on the side effects of en-masse distalization/mesialization of the maxillary dentition, include loss of anchorage, the proclination of anterior teeth, buccal inclination of the posterior segment, and risk of high forces on periodontal ligament which could lead to periodontal breakdown. (Whyte et al, 2019)

The density of the maxilla and the special configuration of the anterior alveolar process are important for a balanced facial profile. The dental substrate of the alveolar process plays a role in determining facial appearance. Flaring of the maxillary incisors can be compensated for by retraction of the maxillary incisors to some degree (Drsheraz et al, 2024).

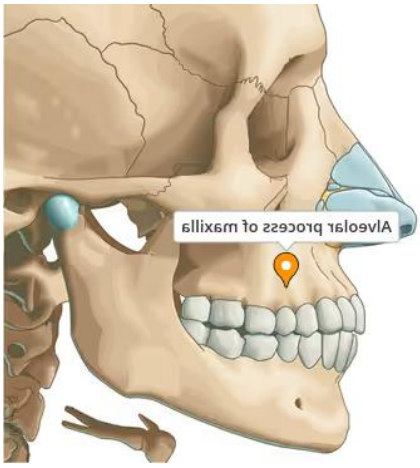

Figure 2.11: Alveolar process on the labial/buccal portion of the maxilla

Figure 2.12: Palatine cortical bone at the level of the palatine vault, and trabecular bone which can be seen around the dentition inside the dental sockets

2.2.2 Biomechanics of Tooth Movement

Proper knowledge acquisition of orthodontic biomechanics began in the 1960s with the pioneering research of Burstone, followed by contributions from Nikolai. Currently, the Finite Element Modeling (FEM) is an effective and efficient approach in studying and quantifying biomechanics and their effects on the dentition and its

surrounding structures. This method offers a diverse array of applications, and in the context of orthodontics, it proves beneficial in several aspects (Reddy & al., 2019). The biomechanics of orthodontic tooth movement has mainly been studied with in vivo and in vitro methods (Li & al., 2021). In addition, animal studies have contributed to the understanding of tooth movement. All of these methods have contributed in some way to the understanding of the process of tooth movement. The main factors involved in tissue reactions and thus tooth movement include biologic and mechanical factors (Henneman & al., 2008).

Though there is no clear understanding of the various factors involved at the cellular and tissue level of orthodontic tooth movement, it has traditionally been elucidated in mechanical terms where the PDL is seen as an elastic, viscoelastic, or poroelastic structure where the key parameters are displacements in the tooth or bone and the change in time when force is applied (Henneman & al., 2008). The stretching of the PDL, with fluid possibly being squeezed out, or the compression and change in morphology of the osteocyte are seen as essential for the bone resorption and formation process caused by the mechanical stimulus. It is not only the type of tissue reaction, but also the size of the force applied and the duration of application and its interaction with the biological control mechanisms which seem to influence tooth movement (Dastgerdi & al., 2023).

2.3 Finite Element Analysis in Dentistry

2.3.1 Introduction to Finite Element Analysis

Research in various fields of Dentistry requires a methodology that is inexpensive and feasible. Such an approach may perhaps be positioned to help guide researchers in

biomechanics structure in both health and disease states (Reddy & al, 2019). In biomechanical research in the field of re-constructive dentistry, endodontics, orthodontics, prosthodontics, periodontology and implantology the oral environment has been investigated in vitro because of its complexity and inaccessibility to the investigator. Computerized modeling is an effective noninvasive technique to reveal in vivo contact mechanics (Fig. 2.13). Thus, to study stress distribution around the peri-implant bone, several approaches have been currently being employed. Some that can be mentioned include photo elastic model, strain gauge analysis and 3D finite element analysis (FEA). Primarily due to availability of software and capability to establish 3D stresses & strains finite element modeling (FEM) has been considered most preferred (Reddy et al, 2019). Finite element is a powerful tool in computational mechanics used in solving a variety of complex problems of practical interest in science and engineering (Aftabi et al, 2024). Dental biomechanics is important because it helps to understand the performance of both the tooth and jaw under different types of stress. This result can be used to help reduce design errors (Phellan et al, 2021). Since the FEM is precisely quantitative and detailed enough to determinate the physiological reactions that can be occurred in tissues, is possible to anticipate the visualization of these tissue responses through the observation of zones of stress generated from the applied orthodontic mechanics (Knop et al, 2015).

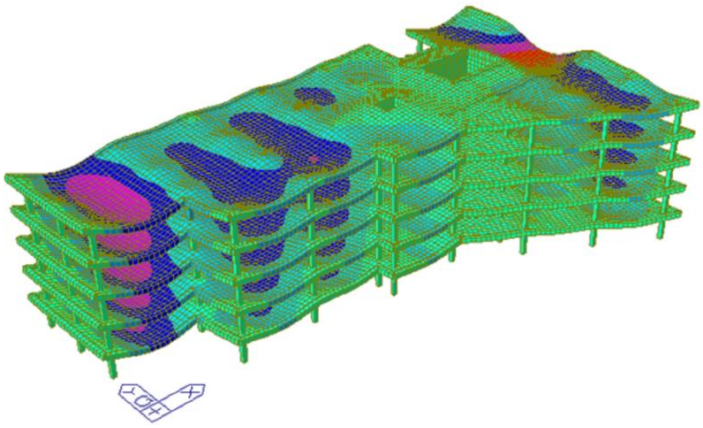

Figure 2.13: FEA of a model building prior to its construction displaying areas of critical stress for its design

2.3.2 Basics of Finite Element Modeling

Finite element models simulate complex situations or structures by solving an intricate boundary-value problem (Phellan et al., 2021). Here, the object under study is divided into a large number of small, geometrically simple sub-objects. The division begins with a mesh or grid, and so elements are produced. These elements are interconnected at specified locations, which constitute a mesh. Interconnections are often the sites of mechanical loading or constraint. At each element, the physical situation is described mathematically by a set of linear or nonlinear equations that satisfy specified boundary conditions. Each material that makes up the modeled situation has its own set of material properties. Collectively, these numerical relationships illustrate the behavior of the structure under the situation's specific applied mechanical load (Reddy & al, 2019).

Finite element models have advantages and disadvantages. The modeling of complex whole-body structures is not possible with present computer capabilities because of the enormous number of finite elements needed. Having to express the geometric configuration of a biological object with a mesh leads to the significant disadvantage of mesh dependency. This is the phenomenon that the movement of one element changes

the response of neighboring elements, which leads to large deformation problems. To a large extent, mesh dependency will always exist. The finite element method is an approximation method that depends on the smallness of the represented elements and the overall model size. Substantial effort goes into mesh convergence studies for the particular problem being modeled to ensure that the results have acceptable precision (Reddy et al, 2019). The model configurations were defined by a mesh. If several prosthetic systems are included in a model, the number of elements and the complexity of the computations are very large. Hence, the study concerns the logical configuration of the model with dose dependency analyses at several stages. Moreover, some of the advantages of FE are the following; it allows for the visualization of overlapping structures, facilitates the assessment of specifications and material properties of craniofacial anatomy, enables the identification of the magnitude and direction of applied forces, provides theoretical measurements of stress points, maintains the physical properties of the materials under analysis, allows for easy repetition of studies, supports both static and dynamic analyses, reduces the time required for studies, and eliminates the need for animal sacrifice to assess stress and strain (Reddy et al, 2019).

On the other hand, the disadvantages of FEM would be; having inaccurate data, statistics, and interpretations which can lead to misleading results, a certain level of computer proficiency is required, comprehensive knowledge of mechanical behaviors is necessary, certain assumptions must be accepted, which means that the outcomes are influenced by the individuals involved in the study, and the resulting quantitative data have hypothetical value and not direct major clinical relevance. Also, the absence of technologies to measure the properties of oral tissues has prevented determination of the correct assumption to simulate the PDL function.

Most dental FEA studies use an isotropic and homogeneous material property for the PDL, which may lead to simplistic and inaccurate outcomes, and FEA studies provide a “snap-shot” of the initial conditions (e.g. stresses, displacement) when the tooth is pushed in the PDL space before the bone resorption/apposition phases, and do not depict changes overtime in the rate of tooth movement, bone remodeling, healing, and friction. Subsequent clinical results may not be similar to the initial ones (Reddy et al, 2019) (Zeno & Ammoury, 2023).

2.3.3 Applications of Finite Element Modeling in Dentistry

In dentistry, finite element modeling is successfully applied in modeling various dental tissues under physiological, pathological, or therapeutic conditions. Some of its representative applications are analyses of stress and strain in hard dental tissues, apical stop preparation, distribution of forces in orthodontics, analysis of tooth sensitivity behavior, bonding efficiency of various dental materials, dental implants of different designs (Fig. 2.14), and the alveolar compact bone, as well as their stability in osteo-synthesis with respect to biomechanical factors, such as initial static compressive and dynamic occlusive loads (Fig. 2.15) using finite element modeling programs (Ammoury et al thesis, 2017).

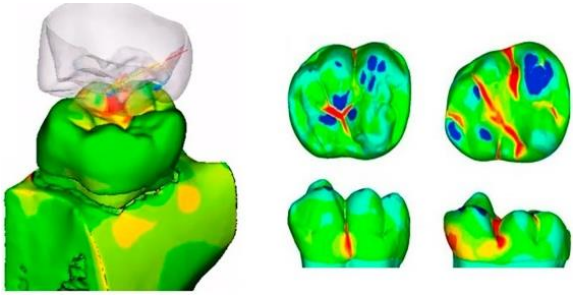

Figure 2.14: FEA of the occlusal surface of molars after occlusion. This helps in identifying any high spots which can cause prematurity when biting.

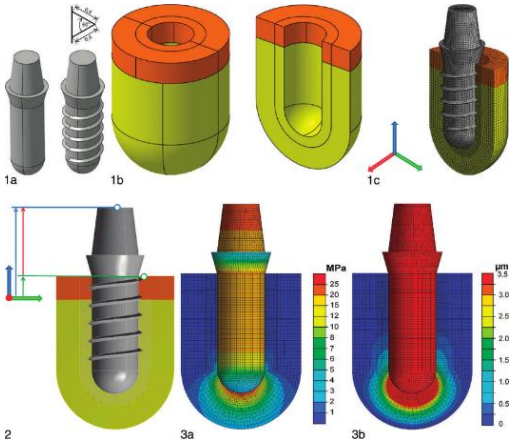

Figure 2.15: A finite element analysis of a dental implant model being subjected to a force and the subsequent stress on the surface and surrounding bone are studied.

2.3.4 Types of 3D Imaging Technologies

Historically, 2D diagnostic imaging records have been conventional for orthodontic analysis although they possess many drawbacks that contributed to the decrease in the reliability of the images as well as not allowing the conversion into 3D models for experimental and clinical studies. Some of these limitations include object magnification, distortion, projective displacement as well as super imposed structures. In the last decade, medicine, then later dentistry embraced 3D technology in the diagnosis and treatment planning (Ammoury et al thesis, 2017).

Several devices utilized for dental diagnostic analyses can produce 3D images. The radiographic techniques can be guided or not guided by computed tomography machines. In addition to CT, other types of imaging can provide 3D imaging using other physical or biological parameters. Nevertheless, some modalities, although not capable of showing 3D, can provide special data on the densities of certain structures, which can be used for simulations in finite element analyses, such as dento-alveolar structures with

or without guided bone regeneration procedures. The reader will understand the different modalities of imaging devices in this section as well as the strengths and limitations of the devices (Ammoury et al thesis, 2017).

Traditional medical tomography, later named computed tomography, was developed as a diagnostic tool in the mid-1970s and was later used in dentistry. By virtue of the image contrast obtained by different densities in tissues through X-ray attenuation in different directions, the device can produce image slices that can be reconstituted in 3D, thus enabling morpho-metric studies and quantitative evaluation of bony tissues. In the analysis, it is important that the section representing slice thickness be smaller than or equal to the voxel size, which in turn is a 3D image element. The more technical data parameters, the better the quality of the radiographic image will be. Currently, the most used CT is the Cone Beam model. Despite the ease of manipulation and reduced execution time in relation to conventional CT, the device does not offer images of structures in soft tissues with as high precision as the latter, although the number of false negatives in diagnoses and the lack of clarity to differentiate between benign and malignant lesions were lower compared with high-resolution conventional CT (Benca et al, 2020).

2.3.5 Applications in Dental Research and Practice

In the last several years, researchers have provided a broad range of FEA applications related to dentistry while highlighting its role in unveiling the biomechanics of dental structures. Singh et al. (2016) identify the use of FEA as a valid and effective approach for examining numerous orthodontic therapies; discuss its application in treatment planning and for illustrating the biomechanics tooth movement. This early

appreciation and recognition mean that subsequent examinations exploring the FEA in various sub-disciplinary areas of dentistry have been possible (Singh et al, 2016).

Building on the discussion, Chang et al. went further to analyze the validation procedures of FEA models in dental implant research. In their informative review, the authors classified a great many of the articles seen by the researchers according to their methods of validation and emphasized that successful validation is of paramount concern to guarantee the credibility of FEA results. Thus, the authors noted that, though FEA has emerged a critical tool for the analysis of the designs for dental implants and the stability of the bones in their proximity, the accuracy of these studies tends to be questionable, thus calling for an integrated validation of such work (Chang et al, 2018).

Cicciù et al (2020) extended this knowledge by focusing on the application of FEA for assessing challenging dental conditions, including orthognathic surgery. His work explained the applicability of finding FEA stress distribution and proved how it can be useful for planning treatment methods strengthening the importance of such tool for dental practice. Ensuring high-resolution imaging is an important requirement explained in this work as being critical to improving precision in FEA uses (Cicciù et al, 2020).

Nevertheless, Lisiak-Myszke et al. (2020) aimed their FEA review to the specialized techniques in oral and maxillofacial surgery. From the presented review they explained how FEA helps in dissecting the mechanical behavior of the human skeleton namely in trauma and reconstructive procedures. They focused on the method of FEA and its ability to explain mechanical interactions that are fundamental to surgical planning and implant design (Lisiak-Myszke et al, 2020).

More recently, Matos et al. (2022) provided a review of bioengineering tools for dentistry wherein FEA received a likewise evaluation. They underlined the need to ensure

proper confirmation of FEA studies are needed because the supporting tissues in the dental structures are inhomogeneous. They also pointed out how FEA could be used in conjunction with other techniques in order to improve the interpretation of occlusal stress and biomechanical behavior in dental practices (Matos et al., 2022).

2.3.6 FEA in Orthodontics

In orthodontics, many questions are challenging to address due to the biomechanical complexity of the stomatognathic system and ethical concerns surrounding the simulation of invasive procedures on human subjects. Computational techniques, such as Finite Element Analysis (FEA), offer a solution to this dilemma. FEA is a non-invasive and highly accurate method that provides quantitative and detailed data on potential physiological tissue reactions. By applying FEA, it becomes possible to anticipate and visualize tissue responses by observing areas of stress generated by applied orthodontic forces (Fig. 2.16) (Knop et al, 2015).

Tanne et al. (1987) were pioneers in introducing FEA into orthodontics. Early studies focused on single-tooth systems, constructed using average anatomical morphologies, to evaluate stress levels following the application of force (Tanne et al, 1987). With advancements in software and the incorporation of 3D radiographic imaging in dentistry, more complex models have been developed to analyze stress distribution in groups of teeth (Liu et al, 2015).

Kang et al. (2016) examined the impact of maxillary second and third molar eruption on first molar distalization using a force of 150 g delivered by a modified palatal anchorage plate (MPAP), a bone-anchored pendulum, and headgear. The eruption stages were divided into three groups: (1) second molar at the cervical third of the first molar

root; (2) fully erupted second molar; and (3) erupting third molar at the cervical third of the second molar root. No significant differences in displacement were observed among the appliances in stages 2 and 3, indicating that third molars did not impact distalization. In stages 1 and 2, the MPAP produced more root than crown distalization with less mesial-in rotation after the second molar eruption. The bone-anchored pendulum caused distalization with distal-buccal tipping and intrusion; however, in the presence of second molars, buccal tipping and extrusion were more pronounced. Headgear produced the greatest amount of distal tipping of the first molar, accompanied by extrusion and distal-in rotation in all stages (Kang et al, 2016).

Yu et al. (2014) reported that using a palatal plate instead of buccally placed mini-implants resulted in bodily molar movement without tipping or extrusion and minimal displacement of incisors. However, their study had two limitations: the model was constructed from a dentoform without distinguishing between stiff cortical and trabecular bone, thus failing to represent real anatomy, and interactions between teeth were defined at individual contact points, treating all teeth as a single object (Yu et al., 2014).

Finite Element Analysis involves three essential steps: pre-processing, processing, and post-processing. Pre-processing includes creating the geometric model, converting it into finished elements, defining material properties, setting boundary conditions, and configuring the loading. In the post-processing stage, results are analyzed, and conclusions are drawn based on calculated stresses, movements, and strains induced by applied forces (Singh & al., 2016).

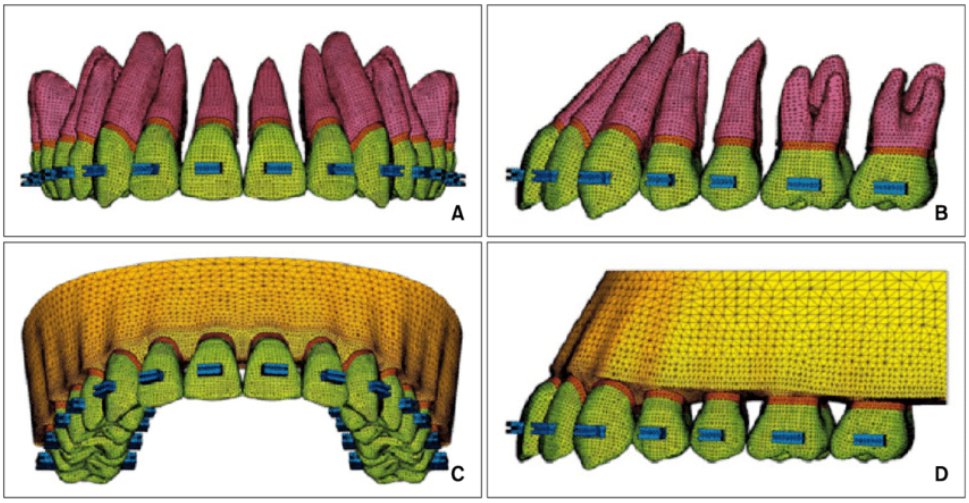

Figure 2.16: FEA of the maxillary dentition during orthodontic treatment

2.4 En-Masse Distalization Techniques

2.4.1 Overview

Distalization of the maxillary dentition is often used in orthodontics to correct Class II malocclusions. Plates, distalizing loops, pendulum appliances, and many different types of headgear have been employed in the past, frequently combined with rapid palatal expansion. En-masse distalization appliances have been employed with increasing frequency in recent years and have the advantage of moving the entire maxillary dentition en-bloc distally over a short period of time, usually without the need for the patient's cooperation (Beyling et al, 2021).

However, distal movement of all teeth, particularly the canines and premolars, also frequently involves bodily tooth movements, which can lead to tilting or extrusion of the incisors during correction of a malocclusion. This can compromise the final result, particularly in closure of an open bite. Forces and moments will come to bear on all teeth in the superstructure of the maxilla, leading to unwanted tooth movements (Bhai et al, 2021). Consequently, clinicians have tried to develop appliances or biomechanics in which the desired distal force is superimposed on the molars only. (Jheon et al, 2013).

2.4.2 Types of En-Masse Distalization Appliance

There are a number of different en-masse distalizing appliances described. They have been creatively designed to bypass a number of treatment difficulties. A major concern found with many en-masse distalization devices in the past is patient compliance. When using extraoral forces or headgear elastics, the patient's compliance is key to the success of treatment (Alogaibi et al, 2021). In 1892 Norman Kingsley provided the first-time description of the headgear, which is useful to maximize distalization of the maxillary molars. The amount of the recommended force is between 150-300 grams which can result in a rate of tooth movement of about 1 mm in a month. Modern appliances utilize TADs for anchorage enable total arch distalization without the risk of anchorage loss. (Singh et al, 2017).

A study by Beyling et al, (2021), evaluates the effectiveness of a new method for treating Class II malocclusions. This method combines maxillary en masse distalization with a completely customized lingual appliance (CCLA) and a novel anchorage concept using mini-screws. The study's goal was to determine if the planned corrections in canine relationship and overjet could be reliably achieved.

The study involved 23 patients, including 3 males and 20 females, with an average age of 29.6 years. Mini-screw anchorage was employed unilaterally or bilaterally across 35 distalization sites. Results showed that 97% of the planned corrections in canine relationship (mean 3.6 mm of 3.7 mm) and overjet (mean 3.1 mm of 3.2 mm) were achieved, both demonstrating statistical equivalence with the treatment plan. The average duration for en masse distalization was 10.5 months, with later cases showing improved efficiency due to refinements in technique. The mechanics used in this method included two mini-screws per side (1 buccal and 1 palatal), elastic chains, and a customized

stainless-steel archwire, which provided enhanced torque control and efficient tooth movement (Beyling et al, 2021).

Modern en-masse appliance designs are very similar in design to previous distalizing appliances using TADs for absolute anchorage. The main difference is that en-masse distalization appliances apply the force on all teeth and enable orthodontic tooth movement of all teeth simultaneously (Fig. 2.17). This is usually done by either crimping or soldering a hook onto a wire or through applying the force on the canine but having the anterior teeth ligated as one unit. Buccal miniscrews could be placed between maxillary first molars and second premolars (interradicular) or infrazygomatic tall (usually around 12 mm) miniscrews can be used.

Figure 2.17 En-masse distalization of the entire maxillary dentition using buccally positioned 6 mm-long inter-radicular miniscrews

Palatal miniscrews can be used as direct anchorage with elastomeric ligatures directed towards the teeth as modified C-palatal plate (Park et al 2017), or as indirect anchorage when used in appliances such as Bone-Anchored Pendulum Appliance (BAPA) (Karvelas et al, 2023), Beneslider, Palatal Skeletal Anchorage System (PSAS) (Wilmes et al, 2010), and in miniscrew assisted distal jet appliance (Kinzinger et al, 2006) (Fig. 2.18).

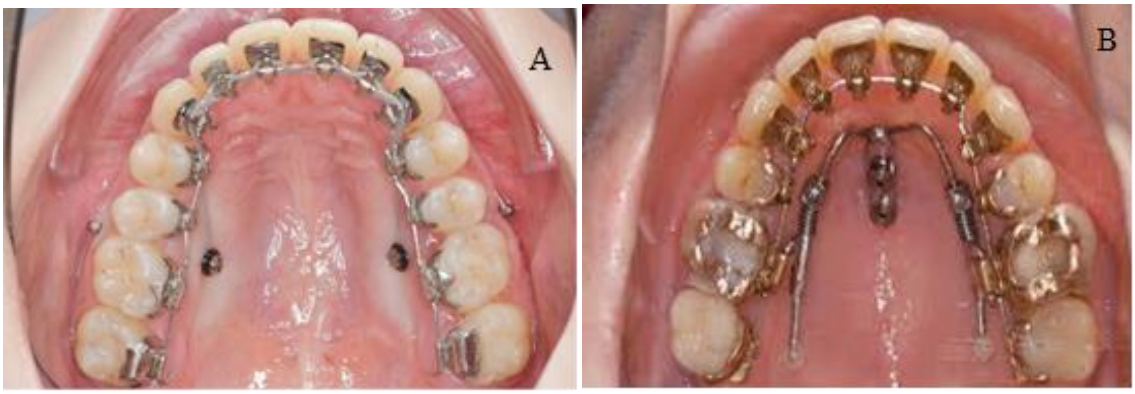

Figure 2.18: En-masse distaliztion of the entire maxillary dentition using palatally positioned miniscrews with: A: direct anchorage, and B: Indirect Anchorage

2.4.3 Force Magnitudes in En-Masse Distalization Studies

In the literature surrounding en-masse distalization of the maxillary dentition, particularly when examined using finite element analysis (FEA) or through clinical studies, there is a noticeable lack of consensus regarding the appropriate force magnitudes to be applied. Studies have reported a wide range of force values, without a standardized approach, which complicates direct comparisons across different research.

For example, in some FEA studies, forces between 50 to 200 grams are often applied to simulate tooth movement (Sujaritwanid et al, 2021), while others, especially in clinical contexts, suggest the use of much higher forces—up to 500 grams or more (Andreasen et al, 1980). This disparity arises from differing objectives, model configurations, and patient-specific variables, leading to inconsistent recommendations on optimal force levels. As a result, while FEA provides precise control and insight into stress distribution, the force values chosen in simulations can significantly differ from those reported in clinical orthodontic practice, where biologic responses and patient comfort are major concerns.

This lack of unification reflects the complexities of studying orthodontic biomechanics, as the force levels required to achieve controlled distalization can vary based on factors such as individual anatomy, appliance design, and treatment goals. Consequently, researchers and clinicians alike face challenges in determining the most effective and appropriate force magnitudes for successful en-masse distalization.

A study by Sujaritwanid et al (2021), indicates that the force magnitudes used for en-masse distalization of the molars range from 200 to 500 grams (approximately 2 to 5 Newtons). In this study, the authors utilize a device (i-Panda) which is anchored by two midpalatal miniscrews and connects to the maxillary molars via a palatal bar. (Sujaritwanid K, 2021).

In another study by Sung et al., the force magnitude used for en-masse distalization is 200 grams. Sung et al. investigated the distalization pattern of the entire maxillary dentition by applying distalizing forces from interdental miniscrews (Sung et al, 2015) (Sung et al, 2010). Sugawara et al. applied a similar distal force of approximately 200 grams per side to the maxillary molars. This force magnitude was selected based on clinical experience and previous studies, aiming to achieve effective molar distalization while minimizing unwanted tooth movements and patient discomfort. Sugawara et al. introduced the Skeletal Anchorage System (SAS) to achieve distal movement of maxillary molars in nongrowing patients. The SAS consists of titanium anchor plates and monocortical screws temporarily placed in the maxilla or mandible, serving as absolute orthodontic anchorage units. (Sugawara & al., 2006)

Kawamura et al. (2017) conducted a biomechanical analysis for total distalization of the maxillary dentition using finite element analysis. They applied a distalization force of 3 newtons (N) to the archwire between the maxillary canine and first premolar at five

different force angulations (FAs): -30°, -15°, 0°, 15°, and 30° relative to the occlusal plane. This approach aimed to identify tooth movement patterns in response to various force vectors. Similarly, in their 2016 study, Chen et al. utilized a force of 3 N for en-masse mandibular dentition distalization. They employed a miniplate-aided skeletal anchorage system to achieve distal movement of the mandibular teeth in a patient with Class III malocclusion (Kawamura, 2017) (Chen et al, 2016).

Jiang et al (2020) compared space closure between loop mechanics and en-masse sliding mechanics using FEA. In their study, they applied an initial retraction force of 125 centi-Newtons (cN) for all three appliances evaluated which is equivalent to about 127 grams of force (Jiang & al., 2020).

A 3D finite element study by Hedayati et al applied a retraction force of 150 grams per side to the anterior teeth during en-masse distalization. Another study by Park et al., utilized the same 150 grams of force per side to distalize the maxillary dentition (Hedayati et al, 2016) (Kang et al, 2016).

In a systematic review and meta-analysis by Raghis et al, the authors analyzed various studies on maxillary total arch distalization using temporary anchorage devices (TADs) for treating Class II malocclusions. The force magnitudes applied in these studies varied, reflecting the absence of a standardized protocol. Some studies utilized forces ranging from 200 to 500 grams per side, while others employed different magnitudes (Raghis et al, 2022).

Another systematic review by Mohamed et al evaluated various studies to assess the effectiveness of miniscrew-supported appliances for maxillary molar distalization. The force magnitudes applied in these studies varied, reflecting the absence of a standardized protocol. Studies included in this systematic review showed forces ranging

from 200 to 400 grams per side (Mohamed et al, 2018). This variability highlights the ongoing need for standardized guidelines to ensure consistency in clinical and research practices, as well as the necessity to determine whether increasing force magnitudes leads to greater displacement or if such increases are clinically insignificant and may jeopardize the PDL due to greater, unwanted stresses.

2.5 Significance

This study offers valuable insights into en-masse maxillary distalization by systematically comparing the stress and displacement patterns between 200g and 300g of force. While the literature presents a wide range of force magnitudes, each asserting its effectiveness, a clear consensus on the optimal force level remains elusive.

A key strength of this study lies in its consideration of individual variations in cortical bone thickness and stiffness—factors that play a crucial role in determining the efficiency and resistance to orthodontic tooth movement.

Another novel aspect of this study is its direct comparison of buccal, bucco-palatal, and palatal force applications—an area that has not been extensively explored in previous research. By systematically evaluating these modalities, we identify the differential responses across the studied dentition, allowing for a more accurate approach to mitigating adverse effects such as excessive stress accumulation and unintended torque. Furthermore, by enhancing our understanding of the displacement-to-stress ratio and anchorage considerations, this study contributes to the optimization of en-masse distalization protocols.

2.6 Specific Objectives

1. Assess stress distribution across the periodontal ligament of the studied dentition under varying force magnitudes (200g vs. 300g) and 3 distalization modalities (buccal, bucco-palatal, palatal).
2. Analyze the displacement patterns of the apices and incisal edges/occlusal surfaces of the studied dentition in response to different force modalities.
3. Determine which force magnitude (200g vs. 300g) produces the greatest extent of distalization (displacement).
4. Compare stress distribution and displacement magnitude in relation to variations in cortical bone properties.
5. Investigate the influence of cortical bone stiffness on stress distribution within the studied dentition and its impact on resistance to tooth movement.
6. Evaluate the interplay between stress, displacement, and force modality in the studied dentition.

CHAPTER 3

MATERIALS AND METHODS

3.1 Materials

The 3D models of the maxillary arch previously created by Ammoury et al (Ammoury et al thesis, 2017) were adapted in our study. These models were initially generated from a pre-treatment cranial CT scan of an adult patient seeking radiologic assessment (at the Department of Radiology at the American University of Beirut Medical Center). The scan disclosed a well-aligned complete dentition, parallel roots, and a Class I occlusion with the midlines on, suggesting a normal occlusion and possibly a previous orthodontic treatment.

The different anatomical variations related to the bone morphology which represent 13 different individuals were incorporated into 13 models (Fig. 3.1). These models differ in the cortical bone thickness at several maxillary regions which are the incisors, premolars and molars and each divided into buccal and palatal sections respectively. In addition, another 12 models were incorporated each having unique stiffness bone qualities also at the same respective regions.

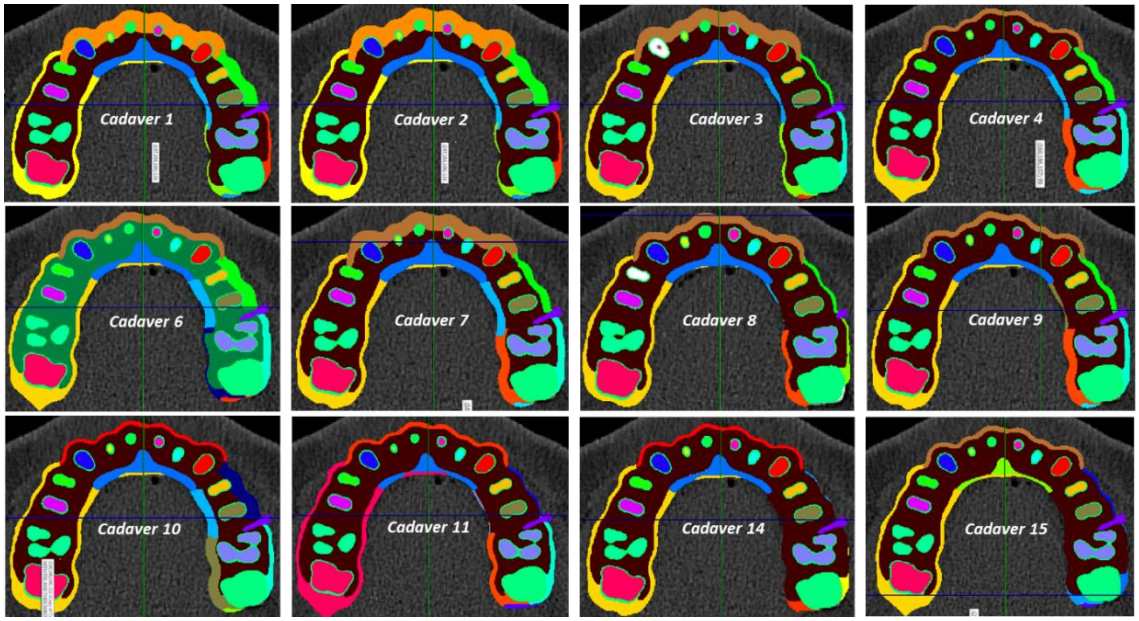

Figure 3.1: TAD level axial cut of the 12 models corresponding to 12 cadavers, based on the initial original model, with modified cortical bone thickness

3.2 Methods

3.2.1 Distalization Setup

Three en-masse distalization setups were introduced. Distalization from buccally positioned miniscrews, palatally positioned miniscrews, and a combination of both. Two distalization forces were applied to the canines; 200 grams and 300 grams. In the bucco-palatal (combined) force modality, the forces were divided into buccal and palatal components to obtain a total of 200 or 300 grams on each side. A total of 39 (13 models with 3 scenarios each) models were used for each force magnitude resulting in a total of 78 models being studied (two force magnitudes for every scenario) for thickness variation. Similarly, a total of 11 models were used for the stiffness variation each undergoing 3 different distalization scenarios and 2 force magnitudes. Therefore, a total of 66 models were studied for the stiffness variation.

All models were modified in ScanIP™ S-2021.06 Build 1266 software (Simpleware, Synopsys, Mountain View, CA, USA). The pre-existing screw was maintained on all models and used as the buccal miniscrew. Another miniscrew was added on the palatal aspect of the maxilla between the maxillary first and second molar. This miniscrew served as the palatal miniscrew. The palatal miniscrew was placed 5 mm from the cemento-enamel junction.

To obtain an accurate replicability, the coordinates (X, Y, Z) of the palatal miniscrew's location on the right side were taken from the original model where the first palatal miniscrew was inserted and then imported to the remaining 12 models. Similarly, after positioning and orienting the palatal miniscrew on the left according to the same criteria as the latter, the (X, Y, Z) coordinates were taken and imported to the remaining 12 models to reproduce the exact same location of all left palatal miniscrews on all the models (Fig. 3.2) (Table 3.1). Moreover, the buccal miniscrew was mirrored on the left side and the coordinates were also replicated on the remaining models. Both sides were included in our study to enable the forces to be directed from both sides to the canines on either side replicating en-masse distalization clinically.

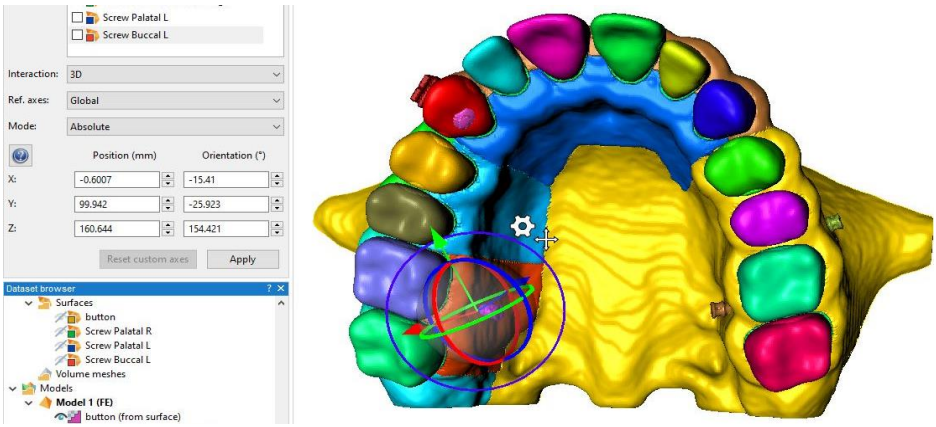

Figure 3.2: TAD positioned on ScanIP™ (Simpleware, Synopsys) module along with its X, Y, & Z coordinates. Each coordinate has a position and orientation in space specified by (mm) and (degrees) respectively.

Table 3.1: coordinates (X, Y, Z) for the position of the miniscrew

	Position (mm)			Orientation (degrees)		
	X	Y	Z	X	Y	Z
Left Buccal Miniscrew	55.635	66.598	155.113	-0.2426	-2.339	134.908
Right Palatal Miniscrew	-0.6007	99.942	160.644	-15.41	-25.923	154.421
Left Palatal Miniscrew	-21.136	48.996	182.779	-48.003	-54.328	-69.155

Moreover, the 3D maxillary model was imported into Solidworks Premium 2015 (Dassault Systèmes, Solidworks Corps, Providence, RI), a 3D modeling computer-aided design software. The button was designed using the Paint 3D software simulating commercially manufactured orthodontics buttons (Fig. 3.3).

Figure 3.3: Palatal button sketched in Paint3D® software

The button was then imported into the ScanIP software as STL file. The button's size and position were modified to have it centered on the palatal aspect of the maxillary right canine through the position and orientation tool (Fig. 3.4).

After positioning the button and miniscrews, the "Surface-to-Mask" option was chosen to convert the button and miniscrews from surfaces to masks. The names of the surfaces to be converted are chosen in the input box and the "Accurate" conversion type was selected. Surfaces are changed to mask to be able to transfer them to model.

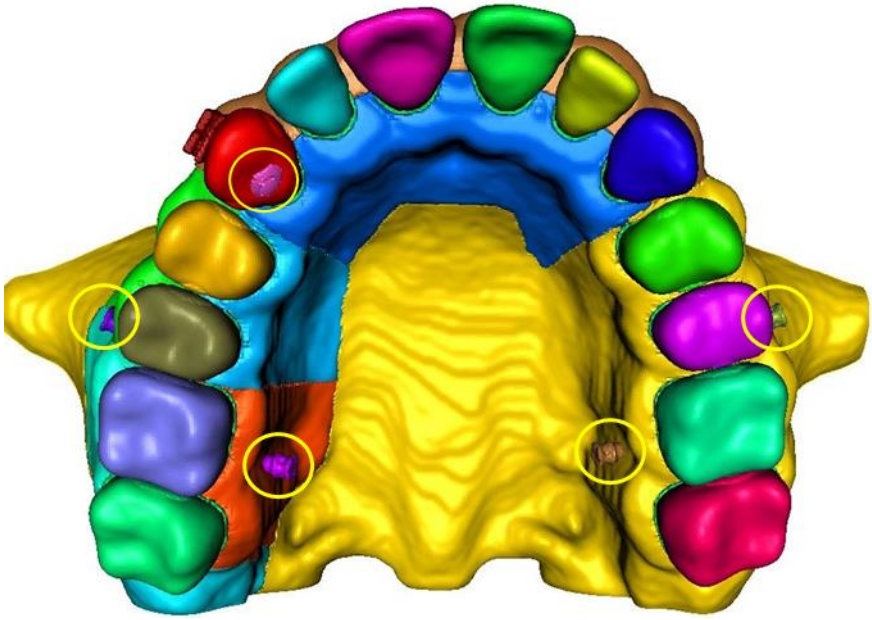

Figure 3.4: 3D model of the final setup of the TADs and the palatal button

3.2.2 Meshing

All the 3D models underwent the process of meshing, which is the discretization of models into elements, in preparation for the finite element analysis. The size of the mesh was set at 0.604 mm (corresponding to coarseness level of -36) following a convergence testing to determine the largest element size at which the results of the solution are similar as previously tested by Ammoury et al (2017). Models were then exported from ScanIP as “inp.” file format.

3.2.3 Finite Element Analysis

The meshed models in the input file format were imported into Abaqus 6.14 (Dassault Systèmes®, Vélizy-Villacoublay, France), a different FEA software.

3.2.4 Material Properties

The material properties (Young's Modulus of Elasticity and Poisson's ratios) of cortical and trabecular bones, teeth, brackets, wires and miniscrews were defined from data available in the literature (Table 3.2). The material property of the PDL was assigned based on the work of Kojima et al (Kojima et al, 2012). All materials used were homogeneous, isotropic, and linearly elastic (Field et al, 2009) (Lim et al, 2003).

Table 3.2: Material properties of various anatomical components commonly used in orthodontic Finite Element Analysis studies (Field et al., 2009; Kojima et al., 2012; Lim et al., 2003).

Material	Young's Modulus (N/mm^2=Mpa)	Poisson's Ratio
Stainless Steel	200,000	0.3
Tooth	20,000	0.2
Cortical Bone	13,700	0.33
Trabecular Bone	1,500	0.33
PDL	0.68	0.45

Cortical bone stiffness was modified according to Peterson et al. (2006) to replicate bone qualities found in real patients. For stiffness variation, unlike other elements of the model, the cortical bone parts were assigned orthotropic material properties providing more detailed information about its behavior under different loads. In material science and solid mechanics, material properties of an orthotropic material differ when measured from different directions.

Each stiffness variation model had different values at 7 different locations, namely the buccal and palatal areas for the incisors, premolars and molars, alongside the tuberosity (Table 3.3). The variation in stiffness for each model was done in Abaqus as previously described by Ammoury et al. (2017).

Table 3.3: Orthotropic material properties at the site of the palatal incisors area

Specimen	Site 1 (Palatal Incisors)								
	E1	E2	E3	V12	V13	V32	G12	G31	G23
1	7720	10762	13809	0.353	0.175	0.426	3021	3783	4545
2	7573	8374	12683	0.429	0.266	0.421	2733	3420	4107
3	8045	10965	11053	0.262	0.368	0.307	3571	3168	2765
4	10254	14545	17301	0.345	0.28	0.318	4193	4587	4981
6	8278.25	11338.08	14088.33	0.339167	0.289583	0.316333	3439.083	3674.167	3909.25
7	11791	16620	18036	0.299	0.373	0.254	5223	4765	4307
9	8278.25	11338.08	14088.33	0.339167	0.289583	0.316333	3439.083	3674.167	3909.25
10	9806	13850	18358	0.384	0.277	0.282	3925	4568	5211
11	7622	12029	13663	0.361	0.35	0.235	3277	3292	3307
14	8278.25	11338.08	14088.33	0.339167	0.289583	0.316333	3439.08	3674.167	3909.25
15	10691	11867	13595	0.208	0.325	0.406	4601	4279	3957

3.2.5 Boundary Conditions

The following boundary conditions were applied in all parts of the study: models were fully constrained in translation and rotation at 2 surfaces of the maxilla superiorly and posteriorly, representing the attachments of the maxilla to its neighboring structures, the zygomatic, palatal, and sphenoid bones. To do so, the "Load" section is chosen in the "Module" dialogue box. The boundary conditions for these areas are chosen as "Encastre" (U1=U2=U3=UR1=UR2=UR3) (Fig. 3.5).

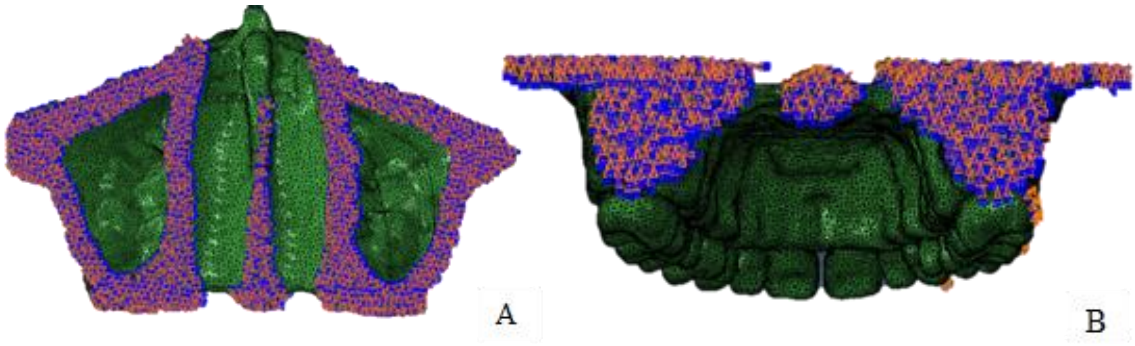

Figure 3.5: Boundary conditions: models constrained from translation and rotation at areas of attachments of the maxilla to adjacent bones: zygomatic, palatal, and sphenoid. A: superior view, and B: posterior view

As for the maxillary dentition, the boundary conditions were chosen as per the areas where the brackets were ought to be placed to mimic the function of the bracket and wire system. This allows the teeth to move in a direction which would be similar to the direction of their movement when loaded in the mouth (Fig. 3.6).

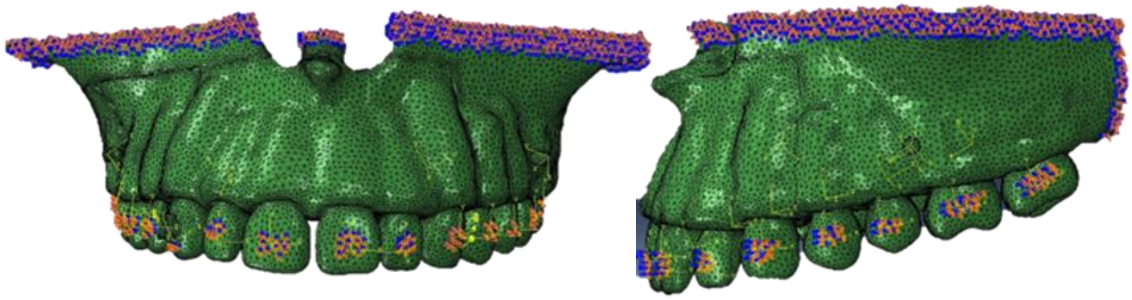

Figure 3.6: Boundary conditions at the level of the maxillary dentition simulating the action of the brackets. A: frontal view showing the BC on the incisors. B: sagittal view showing the BC on the canines, premolars and molars

3.2.6 Interactions

In our method, we used the “surface-to-surface” interaction which assumes the presence of a rigid connection between the teeth without any sliding. Our rationale, mimicking the clinical setting, was that distalization is often applied on a heavy rectangular wire to reduce the distal tipping movement and avoid arch form changes due to the application of force buccal to the center of resistance of the tooth. We chose the “surface-to-surface” interaction for the contact points between the adjacent teeth starting at the distal surface of the canines all the way to the last contact point which is on the mesial surface of the maxillary second molar. In Abaqus the “surface to surface interaction” works only for surfaces in contact with each other. To obtain load transmission through the teeth, adjustments to increase the sensibility of the interactions were needed. Thus, we modified the tolerance of each surface-to-surface interaction to

0.4 or 0.5. As for the anterior teeth, i.e. contact points going from mesial of the right canine to the mesial of the left canine, the interactions were set as “Tie-Constraint” to mimic the action of a ligature or moving the entire maxillary anterior teeth as one unit (which is simulating total arch or en-masse distalization) (Fig. 3.7). The tolerance for the contact points between the anterior teeth were set at 0.7-0.8.

A datum axis system was constructed using 3 points: the origin of the axis system located at the center of the miniscrew head, a second point located at the center of the bracket helped define the X axis, and a third point was placed perpendicular to the X axis. The direction of the direct loading force followed the X axis with no components in the Y and Z axes. As for the canines, premolars and molars, the direction of the forces followed a datum axis system constructed to have the Y axis follow the long axis of each tooth. These forces have only one component in the X axis which is parallel to the archwire. The button on the palatal aspect of the canine followed the same direction as the bracket on the buccal; having only one component in the X axis which is parallel to the archwire. The incisors followed the Y-axis, while the X-axis was parallel to the long axis of the incisors. The interaction property between the teeth was chosen to be frictionless through selecting “Mechanical → Tangential Behavior → Frictionless”.

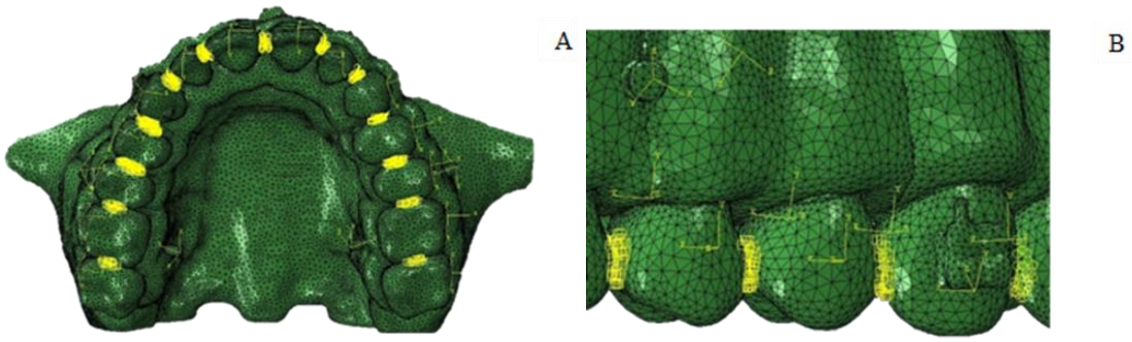

Figure 3.7: A: 3D Model in Abaqus software showing the interactions chosen between the maxillary dentition. B: the different interactions chosen mesial and distal to canine. Mesial to canine "Tie-constraint" interaction was chosen, however, distal to canine "surface-to-surface" interaction was chosen.

3.2.7 Load

The load was placed from the miniscrews to the canine to mimic direct anchorage distalization (Fig. 3.8). Three en-masse distalization modalities were generated for each model and for each force magnitude.

- Buccal force: force was generated from the buccal miniscrew to the bracket on the right canine
- Palatal force: force was generated from the palatal miniscrew to the button on the palatal aspect of the right canine
- Combined Bucco-Palatal force: forces were generated from both buccal and palatal miniscrews to the bracket and button respectively.

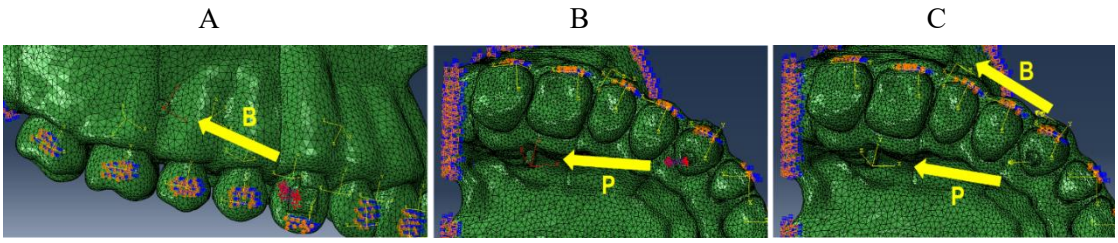

Figure 3.8: The 3 distalization modalities implemented in our study. **A**: buccal force delivered from a buccally positioned TAD. **B**: palatal force delivered from a palatally positioned TAD, and **C:** bucco-palatal force delivered from both buccally and palatally positioned TADs.

As for the variation in force magnitude, two forces were studied: 200 grams (1.96 Newtons) and 300 grams (2.94 Newtons) of force. In the combined modality, the 200 grams-force magnitude were divided into 100 grams (0.98 Newtons) for the buccal force and 100 grams for the palatal force. Similarly, for the 300 grams of force, the forces were split into 150 grams (1.47 Newtons) on either side.

3.2.8 Data Collection and Export

- Measures:

Stress was evaluated at the PDL, and displacement of the crowns were assessed. The stress distribution produced by forces between the periodontal ligament and the bone indicate the location where tooth movement occurs. Therefore, stress at the PDL is assumed be in proportion to the bone-remodeling rate (Kojima et al, 2012). It also infers about the areas that are more prone to root resorption (Zeno et al thesis, 2017). Von Mises stress, evaluated at an element, is a measure of the elasticity of a material, and represents the point at which the elastic limit is exceeded and permanent deformation results. Total displacement includes the sum of the initial translation movements of a node in the X, Y, and Z axes in addition to the rotation movements around the same axes systems.

- Set:

FEA results are usually interpreted by means of color mapped representations and arrows. However, to be able to portray and quantify individual variations, statistical analysis applied on numerical data is required. Abaqus offers the possibility to collect numerical stresses, displacement and other phenomena at each node or element. For stress data collection, a set containing randomly selected elements uniformly dispersed along each surface of the periodontal ligament was created. For each scenario, in each model, i.e. buccal, palatal or the combined modality, the teeth chosen to have the stresses studied on were the incisors, canines and first molars. For each tooth, 8 different sets were created, 3 on the buccal, 3 on the palatal and 1 on each of the proximal sides. The sets created are shown in the figure 3.9.

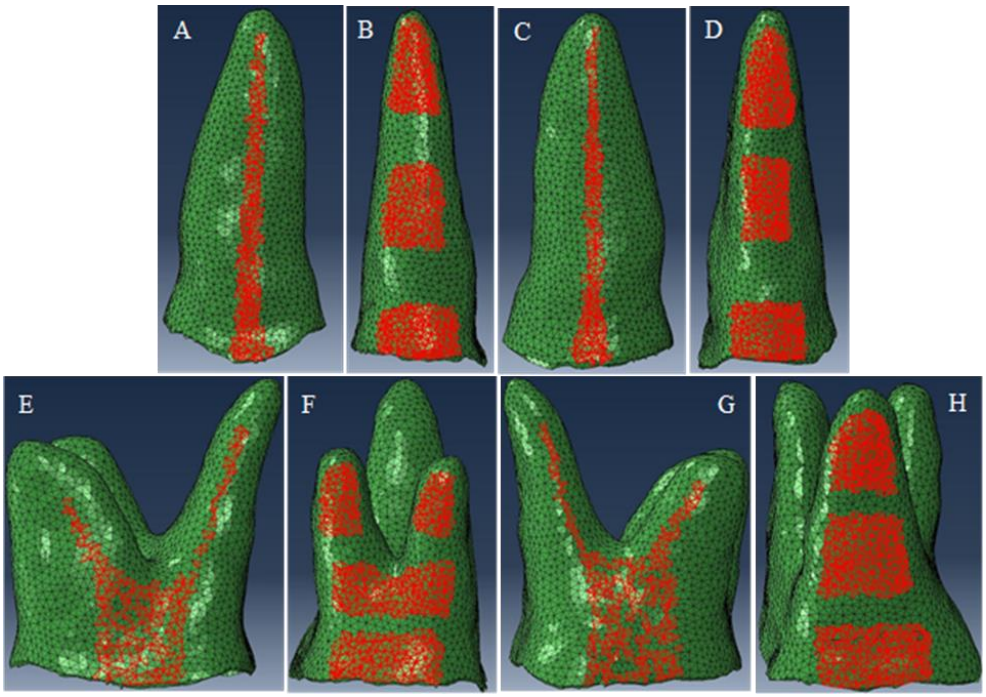

Figure 3.9: Selected elements on A: mesial, B: buccal, C: distal and D: palatal aspect of the maxillary canine, and similarly selected elements of E: mesial, F: buccal, G: distal, and H: palatal aspect of the maxillary first molar. These areas represent areas where stresses are to be measured and quantified.

For displacement data collection, sets of nodes were selected. The number of nodes for each set was between 10 and 18 (depending on the tooth and surface area). For each tooth, 2 sets of nodes were created, first being on the tip of the crown and the second being on the tip of the apex (Figs. 3.10 & 3.11 & 3.12). This allowed us to study the manner of movement of the teeth. The resulting sets were used to measure the initial displacement.

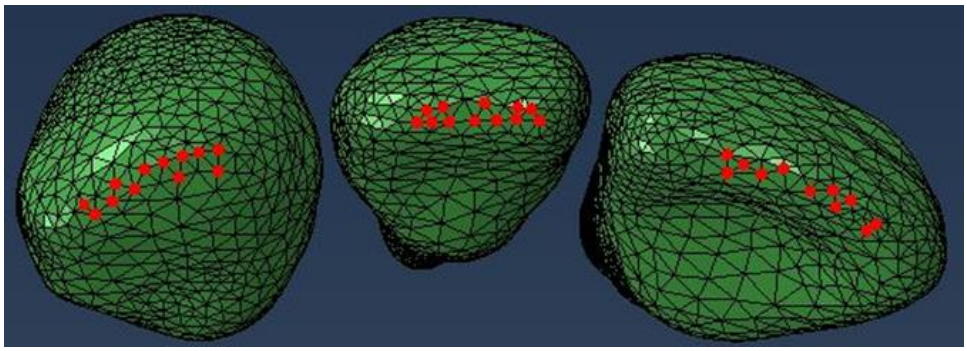

Figure 3.10: Nodes chosen on the incisal tips of the canines, lateral incisors and central incisors. These nodes represent areas where displacement will be measured.

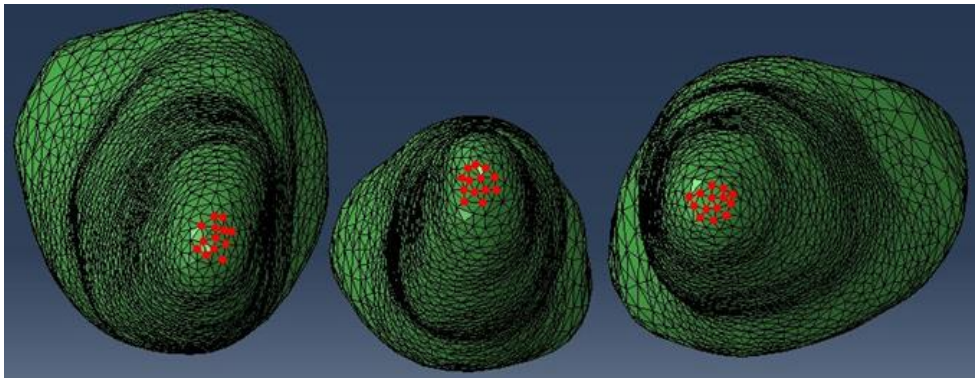

Figure 3.11: Nodes chosen on the apices of the canines, lateral incisors and central incisors.

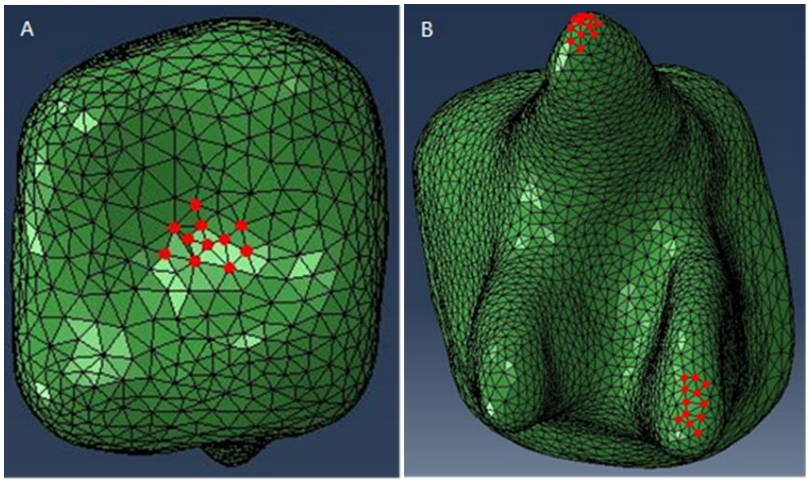

Figure 3.12: Nodes selected on the A: occlusal surface of the maxillary first molar at the centroid region, and B: on the palatal and mesio-buccal roots of the maxillary first molar

To study the displacement of the molar, the centroid of the occlusal surface (center of the occlusal surface) was chosen. To study the displacement at the level of the roots, two sets were created (being multi-rooted): one on the mesio-buccal root and another on the palatal root. This will enable us to study rotations alongside the displacement.

Forces were applied on the right and left sides of the maxilla to accurately represent en-masse distalization, yet, since the maxilla is a mirror image, all data were collected on the right side only.

After running the finite element analysis, the stress and displacement results were exported as “DAT.” files into Excel (Microsoft Excel, Office16, Redmond, WA, USA) where the averages were calculated. Finally, the averages included in the final data sheets. FEA results were also displayed as color mapped representations and arrows for one of the models for visualization of the results. However, to assess individual variations, statistical analysis was applied to the numerical data.

Six data sheets corresponding to the 6 parts of the study were obtained, each containing data for stress and displacement for both 200 and 300 grams of force:

- Part 1: Stiffness variation applied to buccal modality
- Part 2: Stiffness variation applied to palatal modality
- Part 3: Stiffness variation applied to bucco-palatal modality
- Part 4: Thickness variation applied to buccal modality
- Part 5: Thickness variation applied to palatal modality
- Part 6: Thickness variation applied to bucco-palatal modality

3.3 Statistical Analysis

To analyze the stress and displacement data across different modalities (Buccal, Bucco-palatal, and Palatal) and force magnitudes (200 grams and 300 grams), the following statistical approach was employed. Since the data was not normalized, non-parametric statistical tests were used to account for the lack of distribution assumptions. Key statistical methods included the Kruskal-Wallis test for overall comparisons and post hoc pairwise tests for specific group comparisons. Additionally, the significance of differences between groups was evaluated using Analysis of Variance (ANOVA) for certain subsets of the data where approximate assumptions of variance equality were met. Post hoc tests such as Bonferroni corrections were employed to adjust for multiple comparisons.

CHAPTER 4

RESULTS

The results are presented in the following succession: stress on and displacement of teeth under the force magnitude categories (200g and 300 g) and under stiffness and thickness variations, for the various setups (B, BP, P). Von Mises stress values are measured in megapascal (MPa) and displacement values are measured in millimeters (mm).

4.1 Force Magnitude Of 200 Grams

4.1.1 Stiffness Variation

4.1.1.1 Stress

The mean stress values varied significantly across teeth and modalities. All the teeth exhibited the highest stress in the buccal modality, followed by the bucco-palatal and palatal modalities (Table 4.1). In relative comparisons, the highest stress values observed in the buccal setups were at the canine and lateral incisor levels. Statistically significant differences ($0.000<p<0.05$) were observed between all modalities except differences between B and BP ($p=0.069$) and BP and P ($p=0.071$) for the central incisor.

Table 4.1: Comparisons of mean von mises stress generated on the evaluated teeth among treatment modalities

Tooth	Modality	Stresses (MPa)	p			
I1.P	B	4.35×10^{-3}	B		BP	0.069
	BP	3.04×10^{-3}	BP	vs	P	0.071
	P	1.73×10^{-3}	P		B	0.000
I2.P	B	5.65×10^{-3}	B		BP	0.030
	BP	3.84×10^{-3}	BP	vs	P	0.042
	P	2.13×10^{-3}	P		B	0.000
C.D	B	6.07×10^{-3}	B		BP	0.008
	BP	3.74×10^{-3}	BP	vs	P	0.051
	P	1.93×10^{-3}	P		B	0.000
M1.D	B	2.47×10^{-3}	B		BP	0.000
	BP	1.72×10^{-3}	BP	vs	P	0.000
	P	9.71×10^{-4}	P		B	0.000

I1: Central incisor, I**2**: Lateral incisor, **C**: Canine, **M1**: First molar, **P**: Palatal surface, **D**: Distal surface

4.1.1.2 Displacement

The buccal modality exhibited the highest values, followed by the bucco-palatal and palatal modalities. Palatal displacement at the central incisor apex in the buccal modality (1.78×10^{-3} mm,) was significantly higher than in the bucco-palatal (1.27×10^{-3} mm) and palatal (7.63×10^{-4} mm) modalities (Table 4.2). Displacement at the incisal edge followed a similar trend; however, the amount of palatal displacement was greater than at the apex. The same patterns were also observed at the lateral incisor and canine, although the canine apex demonstrated a unique behavior, displacing in an opposite direction (forward) under the palatal modality, (-4.39×10^{-4} mm). Statistical analysis confirmed significant differences across modalities, particularly between buccal and palatal setups.

Table 4.2: Comparisons of mean displacement generated on the evaluated teeth among treatment modalities

Tooth	Modality	Displacement (mm)	p			
I1.a	B	1.78×10^{-3}	B		BP	0.277
	BP	1.27×10^{-3}	BP	vs	P	0.277
	P	7.63×10^{-4}	P		B	0.005
I1.i	B	6.21×10^{-3}	B		BP	0.000
	BP	4.34×10^{-3}	BP	vs	P	0.000
	P	2.46×10^{-3}	P		B	0.000
I2.a	B	2.72×10^{-3}	B		BP	0.097
	BP	2.01×10^{-3}	BP	vs	P	0.097
	P	1.30×10^{-3}	P		BP	0.000
I2.i	B	4.89×10^{-3}	B		BP	0.000
	BP	3.53×10^{-3}	BP	vs	P	0.000
	P	2.16×10^{-3}	P		B	0.000
C.a	B	1.98×10^{-3}	B		BP	0.001
	BP	7.69×10^{-4}	BP	vs	P	0.001
	P	-4.39×10^{-4}	P		B	0.000
C.i	B	4.23×10^{-3}	B		BP	0.000
	BP	3.07×10^{-3}	BP	vs	P	0.000
	P	1.91×10^{-3}	P		B	0.000
M1.a.mb	B	1.78×10^{-3}	B		BP	0.000
	BP	1.24×10^{-3}	BP	vs	P	0.000
	P	7.00×10^{-4}	P		B	0.000
M1.a.p	B	8.51×10^{-4}	B		BP	0.000
	BP	5.89×10^{-4}	BP	vs	P	0.000
	P	3.27×10^{-4}	P		B	0.000
M1.occ	B	2.94×10^{-3}	B		BP	0.000
	BP	2.04×10^{-3}	BP	vs	P	0.000
	P	1.13×10^{-3}	P		B	0.000

I1: Central incisor, I**2**: Lateral incisor, **C**: Canine, **M1**: First molar, **a**: apex, **i**: Incisal edge, **mb**: mesio-buccal root, **p**: palatal root, **occ:** occlusal surface

4.1.2 Thickness Variation

4.1.2.1 Stress

The von Mises stress patterns under a 200-gram force demonstrated notable variations across teeth and modalities. In the central and lateral incisors, the buccal modality consistently exhibited the highest stress, followed by the bucco-palatal and palatal modalities (Table 4.3). Stress differences were more pronounced in the lateral incisor. While the buccal modality maintained the highest stress on the canine, values across modalities were more evenly distributed compared to the incisors. The first molar

showed the lowest stress among all teeth, although the buccal modality remained the dominant contributor.

Relatively uniform stresses at the central incisor and first molar were not statistically significantly different among modalities. Significant differences were observed for the lateral incisor and canine, particularly between the buccal and palatal modalities.

Table 4.3: Comparisons of mean von mises stress generated on the evaluated teeth among treatment modalities

Tooth	Modality	Stress (MPa)	p			
I1.P	B	2.2051×10^{-3}	B		BP	0.336
	BP	2.0894×10^{-3}	BP	vs	P	0.336
	P	1.8263×10^{-3}	P		B	0.336
I2.P	B	2.8559×10^{-3}	B		BP	0.169
	BP	2.5639×10^{-3}	BP	vs	P	0.169
	P	2.1198×10^{-3}	P		B	0.006
C.D	B	2.7250×10^{-3}	B		BP	0.011
	BP	2.0651×10^{-3}	BP	vs	P	0.731
	P	2.0108×10^{-3}	P		B	0.028
M1.D	B	1.2935×10^{-3}	B		BP	0.684
	BP	1.2454×10^{-3}	BP	vs	P	0.684
	P	1.0980×10^{-3}	P		B	0.684

I1: Central incisor, I**2**: Lateral incisor, **C**: Canine, **M1**: First molar, **P**: Palatal surface, **D**: Distal surface

4.1.2.2 Displacement

Displacement patterns varied across the teeth and modalities, with the buccal modality consistently exhibiting the highest values, followed by the bucco-palatal and palatal modalities (Table 4.4). At the central and lateral incisor apices, displacements were modest, while values at the incisal edges were significantly higher across all modalities. The canine demonstrated a unique response, with the apex showing a negative displacement under the palatal modality, indicating movement in the opposite direction.

The first molar exhibited the lowest displacements, particularly at the palatal root, reflecting the dissipation of forces across the broader dentition.

Table 4.4: Comparisons of mean displacement generated on the evaluated teeth among treatment modalities

Tooth	Modality	Displacement (mm)	p			
I1.a	B	7.2121×10^{-4}	B		BP	0.327
	BP	6.4279×10^{-4}	BP	vs	P	0.122
	P	5.5591×10^{-4}	P		B	0.011
I1.i	B	3.2539×10^{-3}	B		BP	0.411
	BP	2.9899×10^{-3}	BP	vs	P	0.411
	P	2.7205×10^{-3}	P		B	0.411
I2.a	B	1.3398×10^{-3}	B		BP	0.342
	BP	1.2184×10^{-3}	BP	vs	P	0.342
	P	1.0919×10^{-3}	P		B	0.342
I2.i	B	2.3302×10^{-3}	B		BP	0.972
	BP	2.2520×10^{-3}	BP	vs	P	0.972
	P	2.2012×10^{-3}	P		B	0.972
C.a	B	1.0560×10^{-3}	B		BP	0.017
	BP	3.5127×10^{-4}	BP	vs	P	0.002
	P	-6.7069×10^{-4}	P		B	0.000
C.i	B	2.2268×10^{-3}	B		BP	0.989
	BP	2.1389×10^{-3}	BP	vs	P	0.989
	P	2.0463×10^{-3}	P		B	0.989
M1.a.mb	B	8.7917×10^{-4}	B		BP	0.785
	BP	8.1879×10^{-4}	BP	vs	P	0.785
	P	7.4964×10^{-4}	P		B	0.785
M1.a.p	B	5.9979×10^{-4}	B		BP	0.867
	BP	5.6104×10^{-4}	BP	vs	P	0.867
	P	5.1477×10^{-4}	P		B	0.867
M1.occ	B	1.4861×10^{-3}	B		BP	0.551
	BP	1.3729×10^{-3}	BP	vs	P	0.551
	P	1.2477×10^{-3}	P		B	0.551

I1: Central incisor, I**2**: Lateral incisor, **C**: Canine, **M1**: First molar, **a**: apex, **i**: Incisal edge, **mb**: mesio-buccal root, **p**: palatal root, **occ:** occlusal surface

Statistical analysis revealed no significant differences in displacement for most regions, including the central and lateral incisors as well as the first molar. However, the canine apex displayed significant differences, particularly between the buccal and palatal modalities.

4.2. Force Magnitude of 300 Grams

4.2.1 Stiffness Variation

4.2.1.1 Stress

The buccal modality consistently exhibited the highest stress across all teeth, followed by the bucco-palatal and palatal modalities (Table 4.5). The canine demonstrated the highest stress among all teeth, at the buccal to and bucco-palatal modalities. Statistical analysis revealed significant differences in stress distribution between palatal and both buccal and bucco-palatal modalities, but not between the latter.

Table 4.5: Comparisons of mean von mises stress generated on the evaluated teeth among treatment modalities

Tooth	Modality	Stress (MPa)	p			
I1.P	B	6.5183×10^{-3}	B		BP	0.149
	BP	4.5530×10^{-3}	BP	vs	P	0.046
	P	2.5980×10^{-3}	P		B	0.000
I2.P	B	8.4724×10^{-3}	B		BP	0.245
	BP	5.7642×10^{-3}	BP	vs	P	0.028
	P	3.1889×10^{-3}	P		B	0.000
C.D	B	9.0985×10^{-3}	B		BP	0.092
	BP	5.6030×10^{-3}	BP	vs	P	0.032
	P	2.8948×10^{-3}	P		B	0.000
M1.D	B	3.7074×10^{-3}	B		BP	0.212
	BP	2.7061×10^{-3}	BP	vs	P	0.008
	P	1.4562×10^{-3}	P		B	0.000

I1: Central incisor, I**2**: Lateral incisor, **C**: Canine, **M1**: First molar, **P**: Palatal surface, **D**: Distal surface

4.2.1.2 Displacement

Displacement patterns demonstrated dominance of the buccal modality, followed by the bucco-palatal and palatal modalities (Table 4.6) (Fig.4.1). In the central and lateral incisors, displacements were markedly higher at the incisal edges compared to the apices. In contrast, the canine exhibited negative (forward) displacement at the apex under the

palatal modality. Displacement in the first molar was notably lower, particularly at the palatal root apex.

Table 4.6: Comparisons of mean displacement generated on the evaluated teeth among treatment modalities

Tooth	Modality	Displacement (mm)	p			
I1.a	B	2.6639×10^{-3}	B		BP	0.352
	BP	1.9042×10^{-3}	BP	vs	P	0.128
	P	1.1445×10^{-3}	P		B	0.001
I1.i	B	9.3154×10^{-3}	B		BP	0.069
	BP	6.5064×10^{-3}	BP	vs	P	0.015
	P	3.6974×10^{-3}	P		B	0.000
I2.a	B	4.0798×10^{-3}	B		BP	0.222
	BP	3.0151×10^{-3}	BP	vs	P	0.074
	P	1.9505×10^{-3}	P		B	0.000
I2.i	B	7.3414×10^{-3}	B		BP	0.058
	BP	5.2891×10^{-3}	BP	vs	P	0.015
	P	3.2368×10^{-3}	P		B	0.000
C.a	B	2.9657×10^{-3}	B		BP	0.082
	BP	1.1534×10^{-3}	BP	vs	P	0.069
	P	-6.5889×10^{-4}	P		B	0.000
C.i	B	6.3503×10^{-3}	B		BP	0.026
	BP	4.6063×10^{-3}	BP	vs	P	0.021
	P	2.8623×10^{-3}	P		B	0.000
M1.a.mb	B	2.6667×10^{-3}	B		BP	0.023
	BP	1.8583×10^{-3}	BP	vs	P	0.023
	P	1.0499×10^{-3}	P		B	0.000
M1.a.p	B	1.2769×10^{-3}	B		BP	0.049
	BP	8.8393×10^{-4}	BP	vs	P	0.015
	P	4.9092×10^{-4}	P		B	0.000
M1.occ	B	4.4064×10^{-3}	B		BP	0.023
	BP	3.0530×10^{-3}	BP	vs	P	0.023
	P	1.6996×10^{-3}	P		B	0.000

I1: Central incisor, I**2**: Lateral incisor, **C**: Canine, **M1**: First molar, **a**: apex, **i**: Incisal edge, **mb**: mesio-buccal root, **p**: palatal root, **occ:** occlusal surface

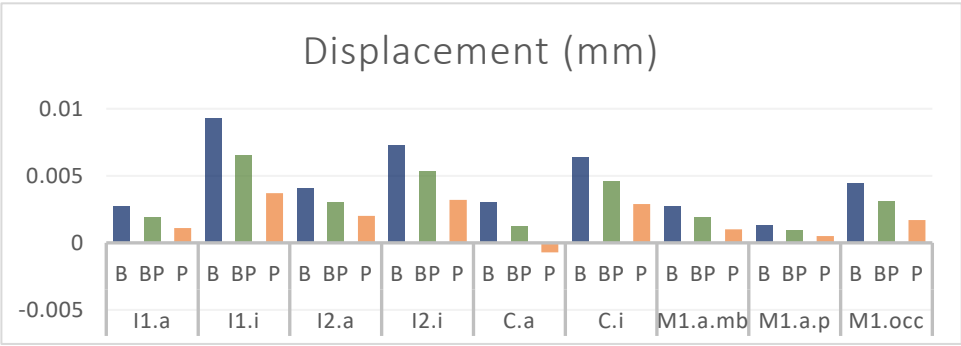

Figure 4.1: Graphic representation of data in Table. 4.6

The most consistent statistically significant differences across all teeth were between the palatal and buccal modalities, followed by the differences between palatal and bucco-palatal modalities. Specifically, the significant differences were observed at the incisal edges of the central incisors, lateral incisors, and canine. Conversely, no statistically significant differences were detected between the buccal and bucco-palatal modalities at the apices of the incisors and canine. The first molar exhibited significant differences across all modalities, particularly at the mesio-buccal apex, palatal root apex, and occlusal surface.

4.2.2Thickness Variation

4.2.2.1 Stress

In a recurring pattern, the buccal modality generating the highest mean stress, followed by the bucco-palatal and palatal modalities. The difference between the bucco-palatal and palatal modalities was less pronounced in the canine than at the incisors (Table 4.7). Stresses in the first molar were comparatively lower across all modalities. The only statistically significant differences among modalities were observed between palatal and buccal modalities at the lateral incisors and canine.

Table 4.7: Comparisons of mean von mises stress generated on the evaluated teeth among treatment modalities

Tooth	Modality	Stress (MPa)	p			
I1.P	B	3.3166×10^{-3}	B		BP	0.295
	BP	2.9529×10^{-3}	BP	vs	P	0.295
	P	2.7484×10^{-3}	P		B	0.295
I2.P	B	4.3166×10^{-3}	B		BP	0.056
	BP	3.5945×10^{-3}	BP	vs	P	0.502
	P	3.2228×10^{-3}	P		B	0.010
C.D	B	4.0965×10^{-3}	B		BP	0.058
	BP	2.8539×10^{-3}	BP	vs	P	0.286
	P	3.1097×10^{-3}	P		B	0.003
M1.D	B	1.9491×10^{-3}	B		BP	0.628
	BP	1.7923×10^{-3}	BP	vs	P	0.628
	P	1.6559×10^{-3}	P		B	0.628

I1: Central incisor, I**2**: Lateral incisor, **C**: Canine, **M1**: First molar, **P**: Palatal surface, **D**: Distal surface

4.2.2.2 Displacement

Displacement patterns followed a parallel distribution to stress, the buccal modality yielding the highest values, followed by the bucco-palatal and palatal modalities (Table 4.8) (Fig. 4.2). In the central and lateral incisors, displacements were markedly higher at the incisal edge compared to the apex. A negative (forward) displacement at the canine apex was exhibited under the palatal modality. The first molar demonstrated the lowest displacement overall, particularly at the palatal root. The only statistically significant differences were between palatal and buccal modalities at the apex of the central incisor, and between palatal and either buccal and bucco-palatal setups at the apex of the canine.

Table 4.8: Comparisons of mean displacement generated on the evaluated teeth among treatment modalities

Tooth	Modality	Displacement (mm)	p			
I1.a	B	1.0753×10^{-3}	B		BP	0.327
	BP	9.9437×10^{-4}	BP	vs	P	0.122
	P	8.6082×10^{-4}	P		B	0.011
I1.i	B	4.9492×10^{-3}	B		BP	0.411
	BP	4.5520×10^{-3}	BP	vs	P	0.411
	P	4.1424×10^{-3}	P		B	0.411
I2.a	B	1.9747×10^{-3}	B		BP	0.342
	BP	1.8872×10^{-3}	BP	vs	P	0.342
	P	1.6917×10^{-3}	P		B	0.342
I2.i	B	3.5664×10^{-3}	B		BP	0.972
	BP	3.4348×10^{-3}	BP	vs	P	0.972
	P	3.3265×10^{-3}	P		B	0.972
C.a	B	1.6015×10^{-3}	B		BP	0.017
	BP	3.7701×10^{-4}	BP	vs	P	0.002
	P	-9.2474×10^{-4}	P		B	0.000
C.i	B	3.4432×10^{-3}	B		BP	0.989
	BP	3.2473×10^{-3}	BP	vs	P	0.989
	P	3.1024×10^{-3}	P		B	0.989
M1.a.mb	B	1.3855×10^{-3}	B		BP	0.785
	BP	1.2423×10^{-3}	BP	vs	P	0.785
	P	1.1356×10^{-3}	P		B	0.785
M1.a.p	B	9.5212×10^{-4}	B		BP	0867
	BP	8.5213×10^{-4}	BP	vs	P	0.867
	P	7.7969×10^{-4}	P		B	0.867
M1.occ	B	2.3050×10^{-3}	B		BP	0.551
	BP	2.0848×10^{-3}	BP	vs	P	0.551
	P	1.8964×10^{-3}	P		B	0.551

I1: Central incisor, I**2**: Lateral incisor, **C**: Canine, **M1**: First molar, **a**: apex, **i**: Incisal edge, **mb**: mesio-buccal root, **p**: palatal root, **occ:** occlusal surface

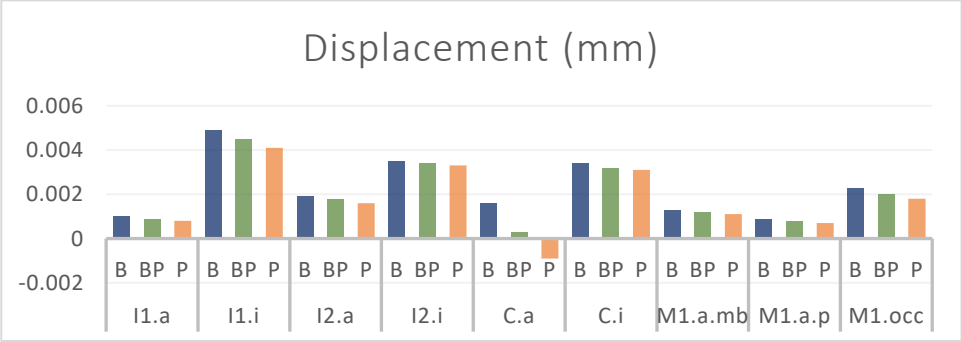

Figure 4.2: Graphic representation of data in Table. 4.8

4.3 Comparison of Stress and Displacement Under Variation in Force Magnitude (200 Vs 300g)

The forces evaluated were 200g and 300g, translating in an increase of 50% (300/200 = 1.5). We assessed the ratios of stress (S) values and displacement (D) measures between the force magnitude groups to determine if the ratio of 1.5 applied to these outcome measures (S300/S200 and D300/D200).

4.3.1 Stiffness Variation

The computed ratios exhibited consistency across teeth and modalities, approaching the 1.5 ratio for teeth and modalities (Table 4.9), indicating proportional increases in stress and displacement with increased force magnitude.

The D/S ratios evaluated in the force magnitude groups revealed distinct patterns across teeth and modalities, with notable regional variations. While the ratios exceeded 1 (1.42) under both force groups at the central incisor in all modalities (buccal, bucco-palatal, palatal modalities), they approached 1 at the molars (Table 4.10). The rations were below 1 for the lateral incisor and canine in the buccal and bucco-palatal modalities but reached nearly 1 in the palatal setup.

Table 4.9: Stress and displacement ratios of individual teeth across different modalities compared between force magnitudes (300 vs 200 grams)- under stiffness variation

Stress				Ratio 300/200	Displacement		Ratio 300/200
		200	300	1.5	200	300	1.5
B	I1	4.35	6.52	**1.49**	6.21	9.32	**1.5**
	I2	5.65	8.47	**1.49**	4.89	7.34	**1.5**
	C	6.07	9.10	**1.49**	4.23	6.35	**1.5**
	M1	2.47	3.71	**1.5**	2.94	4.41	**1.5**
BP	I1	3.04	4.55	**1.49**	4.34	6.51	**1.5**
	I2	3.84	5.76	**1.5**	3.53	5.29	**1.49**
	C	3.74	5.60	**1.49**	3.07	4.61	**1.5**
	M1	1.72	2.71	**1.57**	2.04	3.05	**1.49**
P	I1	1.73	2.60	**1.5**	2.46	3.70	**1.5**
	I2	2.13	3.19	**1.49**	2.16	3.24	**1.5**
	C	1.93	2.89	**1.49**	1.91	2.86	**1.49**
	M1	0.97	1.46	**1.5**	1.13	1.70	**1.5**

I1: Central incisor, I**2**: Lateral incisor, **C**: Canine, **M1**: First molar, **B**: Buccal modality, **BP**: Bucco-palatal modality, **P**: Palatal modality

Table 4.10: Displacement to stress (D/S) ratios of individual teeth across different modalities in force magnitude groups (300 vs 200 grams)- under stiffness variation

200				Ratio D/S	300		Ratio D/S
		Stress	Displacement		Stress	Displacement	
B	I1	4.35	6.21	**1.42**	6.52	9.32	**1.42**
	I2	5.65	4.89	**0.86**	8.47	7.34	**0.86**
	C	6.07	4.23	**0.69**	9.10	6.35	**0.69**
	M1	2.47	2.94	**1.19**	3.71	4.41	**1.18**
BP	I1	3.04	4.34	**1.42**	4.55	6.51	**1.43**
	I2	3.84	3.53	**0.91**	5.76	5.29	**0.91**
	C	3.74	3.07	**0.82**	5.60	4.61	**0.82**
	M1	1.72	2.04	**1.18**	2.71	3.05	**1.12**
P	I1	1.73	2.46	**1.42**	2.60	3.70	**1.42**
	I2	2.13	2.16	**1.01**	3.19	3.24	**1.01**
	C	1.93	1.91	**0.98**	2.89	2.86	**0.98**
	M1	0.97	1.13	**1.16**	1.46	1.70	**1.16**

I1: Central incisor, I**2**: Lateral incisor, **C**: Canine, **M1**: First molar, **B**: Buccal modality, **BP**: Bucco-palatal modality, **P**: Palatal modality, **D/S**: Displacement/Stress

4.3.2 Thickness Variation

Similar to the results under stiffness variation, the computed ratios of stresses and displacements within the force groups across teeth and modalities were at or close to the 1.5 ratio for teeth and modalities (Table 4.11).

Table 4.11: Stress and displacement ratios of individual teeth across different modalities compared between force magnitudes (300 vs 200 grams)- under thickness variation

		Stress		Ratio 300/200	Displacement		Ratio 300/200
		200	300	1.5	200	300	1.5
B	I1	2.21	3.32	**1.5**	3.25	4.95	**1.52**
	I2	2.86	4.32	**1.51**	2.33	3.57	**1.53**
	C	2.73	4.10	**1.5**	2.23	3.44	**1.54**
	M1	1.29	1.95	**1.51**	1.49	2.31	**1.55**
BP	I1	2.09	2.95	**1.41**	2.99	4.55	**1.52**
	I2	2.56	3.59	**1.4**	2.25	3.43	**1.52**
	C	2.07	2.85	**1.37**	2.14	3.25	**1.51**
	M1	1.25	1.79	**1.43**	1.37	2.08	**1.51**
P	I1	1.83	2.75	**1.5**	2.72	4.14	**1.52**
	I2	2.12	3.22	**1.51**	2.20	3.33	**1.51**
	C	2.01	3.11	**1.54**	2.05	3.10	**1.51**
	M1	1.10	1.66	**1.5**	1.25	1.90	**1.52**

I1: Central incisor, I**2**: Lateral incisor, **C**: Canine, **M1**: First molar, **B**: Buccal modality, **BP**: Bucco-palatal modality, **P**: Palatal modality

Likewise, the D/S ratios exceeded 1 under both force groups at the central incisor in all modalities (buccal, bucco-palatal, palatal modalities), and approached 1 at the molars (Table 4.12). While the ratios were below 1 for the lateral incisor in the buccal and bucco-palatal modalities, they equaled nearly 1 in the palatal setup. The ratios at the canines were below 1 only under the buccal setup.

Table 4.12: Displacement to stress (D/S) ratios of individual teeth across different modalities in force magnitude groups (300 vs 200 grams)- under stiffness variation

		200		Ratio D/S	300		Ratio D/S
		Stress	Displacement		Stress	Displacement	
B	I1	2.21	3.25	**1.47**	3.32	4.95	**1.49**
	I2	2.86	2.33	**0.81**	4.32	3.57	**0.82**
	C	2.73	2.23	**0.81**	4.10	3.44	**0.83**
	M1	1.29	1.49	**1.15**	1.95	2.31	**1.18**
BP	I1	2.09	2.99	**1.43**	2.95	4.55	**1.54**
	I2	2.56	2.25	**0.87**	3.59	3.43	**0.95**
	C	2.07	2.14	**1.03**	2.85	3.25	**1.14**
	M1	1.25	1.37	**1.09**	1.79	2.08	**1.16**
P	I1	1.83	2.72	**1.48**	2.75	4.14	**1.50**
	I2	2.12	2.20	**1.03**	3.22	3.33	**1.03**
	C	2.01	2.05	**1.01**	3.11	3.10	**0.99**
	M1	1.10	1.25	**1.13**	1.66	1.90	**1.14**

I1: Central incisor, I**2**: Lateral incisor, **C**: Canine, **M1**: First molar, **B**: Buccal modality, **BP**: Bucco-palatal modality, **P**: Palatal modality, **D/S**: Displacement/Stress

4.4 Comparison of Stress and Displacement in Relation to Treatment Modalities

The buccal modality exhibited the highest values across all teeth, followed by the bucco-palatal and palatal modalities. Accordingly, the differences between setups were assessed relative to the buccal values.

4.4.1 Stiffness Variation

Under 200g of force, stress and displacement values for the bucco-palatal and palatal modalities were lower than those recorded under the buccal modality across all teeth (Table 4.13, Fig. 4.3). At the all the teeth, the bucco-palatal setup yielded two-thirds of the stress and displacement observed in the buccal modality; in the palatal setup, the values were less than half of the buccal measures. Similar trends were observed under 300g of force (Table 13, Fig. 4.4). The bucco-palatal modality retained about 70% (range 62% to 73% for stress; 69% to 72.6% for displacement) of the buccal values for both

stress and displacement, while the palatal modality exhibited only 40% (range 38% to 40% for stress; 38.6% to 45% for displacement) at the level of all the teeth.

Table 4.13: Stress and Displacement ($x10^{-4}$) comparison of measurements in BP and P modalities as percentages (%) of B modality under different forces (200 vs 300 grams) (Stiffness variation)

		200 g		300 g		200g		300g	
		Stress	% stress	Stress	% stress	Displ	% displ	Displ	% displ
I1	B	43	-	65	-	62	-	93	-
	BP	30	69.7	45.5	70	43	69	65	70
	P	17	39.5	26	40	24	38	37	40
I2	B	56	-	84	-	48	-	73	-
	BP	38	68	57	68	35	73	53	72.6
	P	21	37.5	32	38	21	44	32	44
C	B	60	-	90	-	42	-	63.5	-
	BP	37	61	56	62	30	71	46	72
	P	19	31.6	28	31	19	45	28.5	45
M1	B	25	-	37	-	29	-	44	-
	BP	17	68	27	73	20	69	30.5	69
	P	10	40	14.5	39	11	38	17	38.6

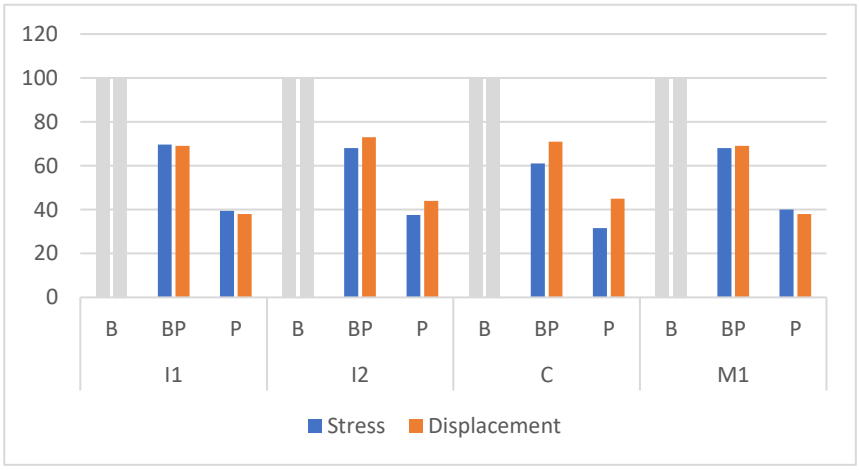

Figure 4.3: Graphic representation of data in Table. 4.13 under 200g of force

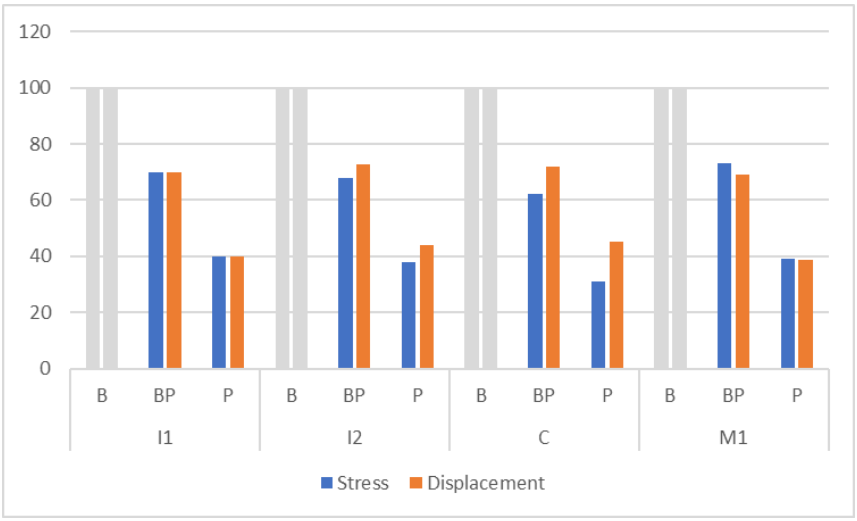

Figure 4.4: Graphic representation of data in Table. 4.13 under 300g of force

4.4.2 Thickness Variation

In the 200g force group, stresses and displacements in the bucco-palatal and palatal modalities were lower at the central incisor than the corresponding buccal measurements by approximately 5% and 18% in stress, and 8% and 17% in displacement, respectively (Table 4.14, Fig. 4.5). Despite lower stress levels at the lateral incisors, the corresponding displacements in the bucco-palatal and palatal were nearly similar to the buccal setup movements (97% and 95%, respectively). The bucco-palatal and palatal modalities at the canine were lower by approximately 26% in stress and up to 10% in displacement but were less pronounced at the first molar.

The same pattern of relativity of stresses and displacements in the bucco-palatal and palatal setups were observed in the 300g group, with observed variations in the differential percentages, e.g. 17% - 18% at the central incisors (Table 4.14, Fig. 4.6).

Table 4.14: Stress and Displacement (x10^{-4}) comparison of measurements in BP and P modalities as percentages (%) of B modality under different forces (200 vs 300 grams) (Thickness variation)

		200 g		300 g		200g		300g	
		Stress	% stress	Stress	% stress	Displ	% displ	Displ	% displ
I1	B	22	-	33	-	32.5	-	49	-
	BP	21	95	29.5	83	30	92	45.5	93
	P	18	82	27	82	27	83	41	83.5
I2	B	28	-	43	-	23	-	35	-
	BP	25	89	36	83	22.5	97	34	97
	P	21	75	32	74	22	95	33	94
C	B	27	-	40	-	22	-	34	-
	BP	20	74	28.5	71.25	21	95	32	94
	P	20	74	31	77.5	20	90	31	91
M1	B	13	-	19	-	15	-	23	-
	BP	12.5	96	18	94	14	93	20	87
	P	11	84	16.5	86	12	80	19	82

B: Buccal modality, **BP**: Bucco-palatal modality, **P**: Palatal modality, **I1**: Central incisor, **I2**: Lateral incisor, **C**: Canine, **M1**: First molar; Displ: displacement

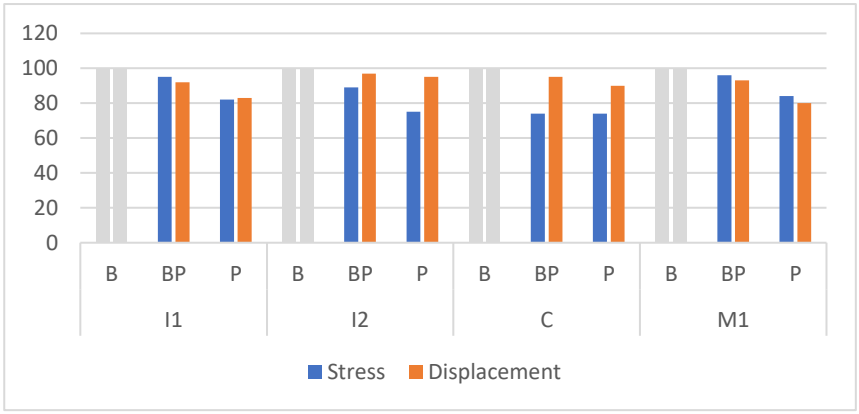

Figure 4.5: Graphic representation of data in Table. 4.14 in the 200g force group

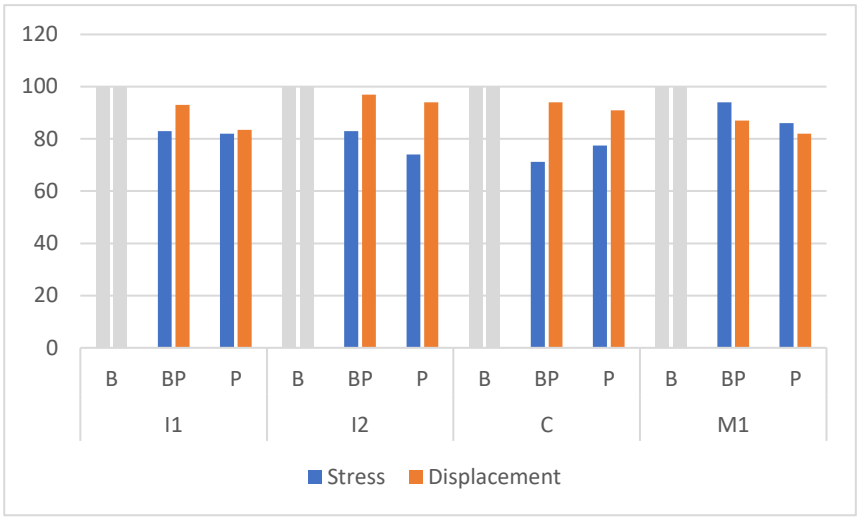

Figure 4.6: Graphic representation of data in Table. 4.14 in the 300g force group

CHAPTER 5

DISCUSSION

The main findings of this study relate to the differential response to distal forces on the anterior (incisors), buccal (canine), and posterior (molar) teeth, the differential gradient of forces (200 vs 300 g) on this response, and the significance of force direction as buccal, bucco-palatal, and palatal. An important component of the findings is the different response of the central incisor from the other teeth, likely because the movement of the central is palatal, while the displacement of the other teeth is predominantly distal. These results and their interpretation are presented in this discussion.

5.1 Differential Response to Distal Forces on Teeth

5.1.1 Stress Analysis

Pairwise comparisons for stress highlighted the significance of the buccal modality's consistently higher values compared to palatal and bucco-palatal modalities. The central incisor exhibited less stress than the canine and the lateral incisor, suggesting that the force level decreased towards the middle of the arch, possibly because of thinner or less dense compact bone at this level.

These findings are consistent with the study by Sung et al. (2015), who utilized a three-dimensional finite element analysis to evaluate stress distribution patterns during maxillary distalization. They reported significant stress accumulation in the canine and lateral incisor regions, and lower stress levels in the molar region, in response to distalizing forces applied via miniscrews. This scheme recurred under different force vectors applied with corresponding variable stress patterns. Our findings also align with the study by Kalia et al. (2019), who evaluated through finite element analysis stress

distribution in the periodontal ligament (PDL) during en-masse retraction of the maxillary anterior dentition (canine to canine) following the extraction of the first premolars. The highest stress levels were observed at the lateral incisor. The authors attributed this finding to the smaller root of the lateral incisor and its intermediate position between the central incisor and canine, which translated into more stress accumulation during distalization. Khan et al. (2021) further supports our observations in a study of stress distribution and displacement patterns in the maxillary arch during distalization against infra- zygomatic screws (IZS). The canine exhibited the highest stress levels, followed by the lateral incisor, then the central incisor. The authors related the differential responses to the canine root morphology and its position in the arch.

5.1.2 Displacement Analysis

The buccal modality exhibited consistently higher values compared to the palatal and bucco-palatal modalities. Specifically, the canine exhibited distinct displacement patterns, whereby the tooth displayed a slight negative displacement of -4.4×10^{-4} at the apex under the palatal modality, leading to palatal crown movement and buccal apex tip. In contrast, the buccal modality produced a positive displacement of 1.98×10^{-3} at the canine apex, effectively achieving outward movement of both the canine cusp and apex. The first molar showed the least displacement, particularly under the palatal modality, with a value of 7.0×10^{-4}.

The central incisor displaced the greatest amount relative to all studied teeth. This finding is corroborated by Song et al. (2016) who also reported the highest displacement at the central incisor during en-masse retraction of the maxillary dentition against buccally positioned orthodontic mini-implants. While their study primarily investigated

the effects of varying mini-implant heights, the displacement findings reinforce the susceptibility of the central incisors to pronounced movement during en-masse distalization. The maxillary distalization study by Khan et al. (2021) using an infrazygomatic screw provides additional support to our findings. Distal displacement values were highest for the central and lateral incisors compared to the canines and molars when measured at a 0 mm lever arm height. The molars showed relatively lesser displacement.

Our findings did not align with those of Lee et al. (2018), who reported greater distalization of maxillary molars when using modified C-palatal plates (MCPP) compared to buccally placed miniscrews. MCPP utilizes indirect anchorage, which may result in a different force application and line of action compared to our setup of direct anchorage applied to the canine using palatally positioned TADs.

Ceratti et al. (2024) conducted a systematic review and meta-analysis to assess the effectiveness of miniscrew-supported maxillary molar distalization. Their analysis revealed that the amount of distalization achieved was not significantly different among palatal (3.74 mm), zygomatic (3.68 mm), and buccal (3.23 mm) TADs. Most of the included studies investigating distalization with palatal modalities utilized either a modified C-palatal plate or similar appliances, whereas others combined buccal miniscrews with various distalizing mechanics. The amount of maxillary first molar distalization achieved with palatal anchorage systems ranged between 1.65 mm and 5.4 mm. The range for buccal anchorage systems was between 2.6 mm and 4.36 mm. These findings highlight the variability in outcomes across studies, which can be attributed to differences in methodologies, appliance designs, and force application protocols.

Discrepancies between findings of various studies highlight the complexity of factors influencing distalization outcomes, including the type of anchorage (direct vs. indirect), appliance design (rigid vs. non-rigid), and the specific mechanics employed. Further research is necessary to delineate the impact of these variables on treatment efficacy.

5.1.3 Displacement-To-Stress Ratios (D/S)

5.1.3.1 D/S Ratios at the Level of the Dentition

The relationship between stress and displacement was assessed in ratios of displacement relative to stress for all teeth. Ratios below 1 indicated that displacement was not concordant with stress, while ratios greater than 1 signified more displacement with less stress. The lateral incisor and canine exhibited a D/S ratio <1 with the buccal modality for both 200 and 300 grams of force and under both stiffness and thickness variations, highlighting the requirement of more stress for displacement (Fig. 5.1). The same pattern was observed for the lateral incisor in the bucco-palatal modality. A nearly 1:1 ratio was observed at the molars in all modalities.

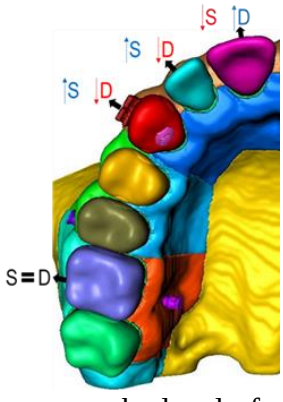

Figure 5.1: Stress and displacement at the level of each tooth with the B modality. The colored areas correspond to the different material properties defined by Peterson et al in the maxilla (Fig. 3.1).

The uniquely different response at the central incisor compared to the lateral incisor, canine, and molar may be related to its central position in the arch, while the proximity of the lateral incisor to the canine explains the corresponding substantial stress values born indirectly from the loads on the canine. Another reason for this distinction may be attributed to the palatal movement of the central versus the distal movement of the other teeth. The density and thickness of the palatal bone opposite the central are relatively lower than in the more posterior zones (Peterson et al, 2006; Fig. 5.2). Accordingly, less resistance to displacement (and higher D/S ratio) may be encountered. In contrast, the canine, distalized into a zone of denser and stiffer cortical bone, would face more resistance, also possibly because of its larger tooth structure. These premises reflect the role of local bone properties in resisting movement.

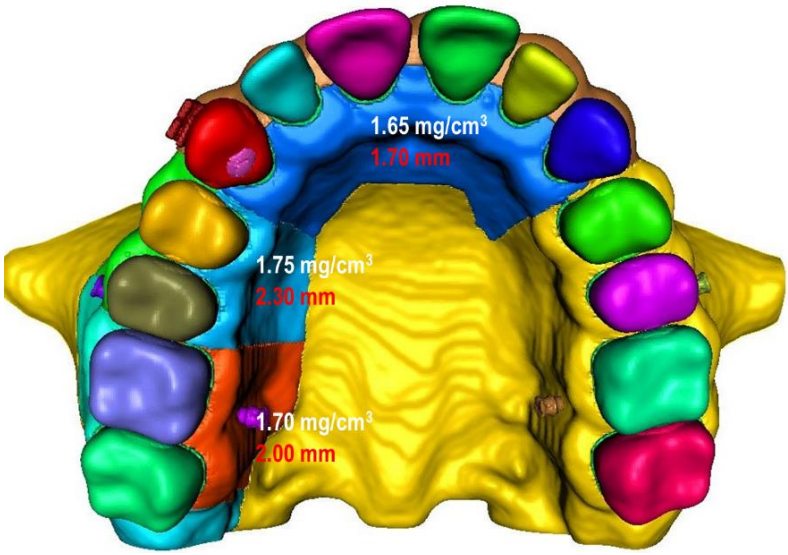

Figure 5.2: Density (in mg/cm^3) and thickness (in mm) of cortical bone at the level of 3 zones: palatal to anterior teeth, palatal to premolars, and palatal to molars (Peterson et al, 2006)

5.1.3.2 Influence of Material Properties

Variations in stiffness influenced the D/S ratio particularly at the level of the canine where the D/S ratio decreased when stiffness was varied. In contrast, variations in thickness resulted in a relatively more balanced interaction between stress and displacement, as evidenced by the D/S ratio of 0.81 under thickness variation compared to 0.61 with stiffness variation in the buccal modality. These results indicate higher stress and displacement values on the maxillary dentition when compared to thickness variation, and that stiffness variation leads to higher stress than displacement. On the other hand, stress and displacement are more evenly distributed under thickness variation, which results in a more moderate response with both stress and displacement reduced in comparison to stiffness variation.

These findings align with the results from Ammoury et al. (2019) who explored the effect of cortical bone stiffness on stress distribution during maxillary tooth distalization. They found that increased cortical bone stiffness resulted in higher stress concentrations in the periodontal ligament (PDL).

5.2 Significance of Force Direction

5.2.1 Comparison of Stress and Displacement Across BP And P As a Function Of B

To better understand the relative advantages or disadvantages of modalities relative to each other, we compared the palatal and bucco-palatal modalities to the buccal setup, which is the commonly used clinical practice. Thus, ratios of the P and BP modalities were computed against the B values for all parameters.

A consistent reduction in stress and displacement was found for both the BP and P modalities compared to the buccal (B) modality, the BP modality frequently

superseding the P modality, demonstrating stress percentages closer to the buccal baseline with higher displacement values. This finding is illustrated in Tables 4.13 and 4.14, whereby P/B percentages are slightly lower than BP/B. This pattern was consistent under variations in stiffness and thickness, and between forces.

The first molar consistently shows lower displacement percentages compared to the canine and central and lateral incisors, particularly in the P modality. Additionally, with stiffness variation, both BP and P modalities show a sharper reduction in stress and displacement percentages compared to thickness variation (Table 4.13 and Table 4.14), with BP still emerging as closer in values to B modality.

5.3 Differential Gradient of Forces (200 Vs 300 G) On Stress and Displacement

When the applied force was increased to 300 g, stress and displacement values rose proportionally by approximately 1.5 times across all modalities and teeth, indicating a direct relationship between force and stress generation.

These findings underscore the importance of careful force modulation during orthodontic treatment. While the proportional increase in stress across all teeth suggests predictable behavior, the higher stress experienced by the canine raises concerns about the potential for overloading with side effects such as pain and root resorption. Clinical research is warranted to determine such outcomes.

5.4 Clinical Implications

The buccal modality was effective for distalization as it generated substantial and potentially fast displacement. However, the concomitant trade-off of higher levels of stress may increase unwarranted side effects (pain, root resorption). In contrast, the

palatal modality generated lower levels of stress and displacement and may provide effective but slower and less damaging movements. However, a potential drawback from the negative torque on the canine may lead to undesirable crown tipping (negative torque) if not prevented by compensatory bends in the wire.

The bucco-palatal modality provided intermediate responses between the B and P setups and may be applied in a variety of clinical situations, particularly when a moderate speed of distalization is desired. Of particular interest is the inference of this research in view of the earlier work by Ammoury et al (2019) and Ghafari and Ammoury (2020). The authors displayed clinical situations where the compact bone slowed down distalization, recommending the use of palatal mini-implants or torque to move teeth away from compact bone into trabecular bone tracks. Our findings support these premises, possibly favoring the bucco-palatal setup, but possibly the palatal setup if proper 3D imaging discloses the site(s) of resistance to distal movement. In summary, matching the individual anatomy with understanding the mechanics and scope of each modality should allow clinicians to select the most appropriate force application based on the specific treatment goals, patient characteristics, and the need to balance movement efficiency with long-term periodontal health.

5.5 Research Considerations

5.5.1 Strengths

5.5.1.1 Evaluation of Different Force Directions

A notable strength is the analysis of full arch (en-masse) distalization compared to most reports about posterior segmental distalization against miniscrews. Moreover, different force systems were compared using different TAD positions: buccal, palatal,

and bucco-palatal. This comprehensive approach not only provided advanced understanding of the interaction between stress and displacement in different anchorage preparations, but also of such interaction when the anterior dentition acted as an additional anchorage setup.

An additional key innovation of this study is the direct evaluation of the displacement-to-stress (D/S) ratio across the studied, disclosing differential responses around the arch and even among teeth categories (e.g. different responses between central and lateral incisors).

5.5.1.2 Consideration of Anatomical and Individual Variations

Another important contribution is the study of clinical setups as they are practiced, not in isolated experimental setups of single teeth or groups of teeth, further strengthened by introducing individual variation in cortical bone thickness and thickness within the anatomy of the maxillary arch. The use of single, standardized models with uniform material properties (bone density, stiffness and thickness) (Kawamura et al, 2021), (Feng et al, 2019), (Sung et al, 2015) does not reflect the potential variation from central tendencies encountered in clinical practice. Variation mechanical properties of bone directly influence tooth movement and stress distribution.

5.5.1.3 Orthotropic Material Properties of Bone

Modeling of bone properties, particularly cortical bone, by using orthotropic material properties to reflect the direction-dependent variations in bone behavior was a departure from most applied finite element modeling, albeit introduced in prior studies by our research group (Ammoury et al, 2019). Earlier studies assumed bone to be

isotropic; more recent research, including studies in orthopedics, has shown that bone is anisotropic (Schwartz-Dabney & Dechow, 2003). As such, bone behaves differently depending on the direction of the applied forces, which can significantly influence stress and strain interactions (Cowin & Hart, 1990). Describing cortical bone as orthotropic, with distinct material properties along three perpendicular axes, offers a more accurate representation of the bone mechanical behavior (Lindh et al., 2004) (Chugh et al., 2013).

Moreover, the introduction of varied mechanical properties as defined by Peterson et al (2006) disclosed variations or zones within the maxilla that influenced the response to distalizing forces differentially. This distinction was further supported in various studies of bone density and thickness when investigating the stability of miniscrews (or even osseointegrated implants) (Bourassa et al, 2018)

5.5.2 Limitations

5.5.2.1 Simplification of the Periodontal Ligament (PDL) Properties

Various approaches exist for modeling the PDL, including linear-elastic, viscoelastic, hyperelastic, and multiphase methods (Fill et al., 2012). However, owing to the limited availability of experimental studies and the absence of advanced technologies to precisely measure the properties of oral tissues, definitive models have not been established to accurately replicate the biological behavior of the PDL. In line with most finite element analysis (FEA) studies in dentistry, this study assumes an isotropic and homogeneous material property for the PDL. While this approach simplifies the modeling process, it may not fully capture the complex biomechanical responses of the PDL, potentially leading to less accurate outcomes (Ammoury et al, 2017).

5.5.2.2 Static Nature of the FEA Model and Challenges in Long-Term Predictions of Tooth Movement

This study provides an initial "snapshot" of stress and displacement patterns immediately following force application, without accounting for the biological changes that occur over time, such as bone remodeling, healing, and frictional effects (Ammoury, Zeno). The results primarily represent the initial displacement of the studied teeth within the PDL space before the subsequent phases of bone resorption and apposition take place.

In clinical settings, the rate and pattern of tooth movement may evolve over time. Roberts et al. (1996) observed that mandibular molar protraction in adult patients decreased from 0.6 mm/month in the first eight months to 0.33 mm/month thereafter. Ideally, a time-dependent (dynamic) FEA model would be necessary to simulate these biological processes and enhance the applicability of FEA in orthodontic treatment planning. Although dynamic FEA models have been proposed since the 1990s (Middleton et al., 1996), replicating the biological processes of orthodontic tooth movement—including PDL and bone remodeling—remains a challenge because to mathematical and computational limitations (Ammar et al., 2011).

While this study simulated the immediate biomechanical response to distalization forces, longer-term effects remain uncertain. Zeno et al. (2020) demonstrated that responses to orthodontic forces can vary significantly depending on the direction of force application, highlighting the importance of patient-specific simulations. Distalization forces, being largely unidirectional, are expected to produce more uniform stress distributions, yet inter-patient variability in long-term outcomes suggests that further refinement of FEA models is needed. The development of time-dependent FEA models incorporating progressive tooth movement and bone adaptation would provide more accurate simulations of clinical reality.

5.5.2.3 Adapted Representation of Individual Variation

Individual variation was incorporated in this study by modifying stiffness and thickness parameters based on a prior study detailing maxillary mechanical properties in human cadavers (Peterson et al. 2006). Ideally, separate CT scans of multiple individuals should be investigated rather than altering the properties of a single model to approximate different anatomical variations. Many authors have used standardized maxillary models and applied uniform force systems, limiting the ability to generalize findings to diverse patient populations. However, our research group has adopted the scheme applied in this research (Ammoury et al., 2019) rather than relying on a single patient's scan with modifications to material properties in lieu of subject-specific anatomical differences (Schwertner et al., 2024).

5.5.2.4 Complexity Of Variability Within Models and Between Individual Measurements

Questions regarding model validity and relations among mechanical properties and displacement are brought up by the finding of greater displacement under stiffness variation than under thickness variation (Figs. 4.1, 4.2). This result defies past findings (Ammoury et al, 2019; Ghafari and Ammoury, 2020) and the principle that stiffer or denser compact bone resists deformation and leads to less displacement.

The reason for this discrepancy laid in the fact that thickness variation was applied under the stiffness value of the original model (SO), which was a high value, whereas stiffness values varied under stiffness variation. To underscore this premise, two specimens were examined under thickness variation: the individuals with least and most amounts of displacement, examined under the SO stiffness value and the lowest stiffness among all cadavers (Peterson et al, 2006). This analysis revealed higher displacement

under low stiffness and lower displacement under higher stiffness (Figs. 5.3, 5.4). These findings reassert the principle of more resistance of stiffer compact bone to tooth displacement, and further support the tenet that stiffness was a more defining property of this resistance.

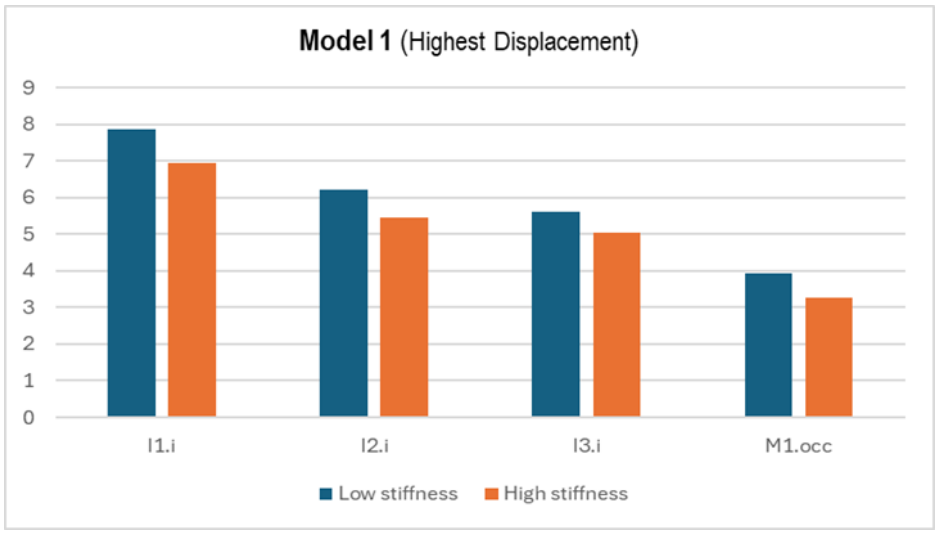

Figure 5.3: The highest displacement (x10^3 mm) under thickness variation, found in the original CT model, subjected to variation in stiffness (high and lowest among all cadavers). Note the greater displacement under low stiffness

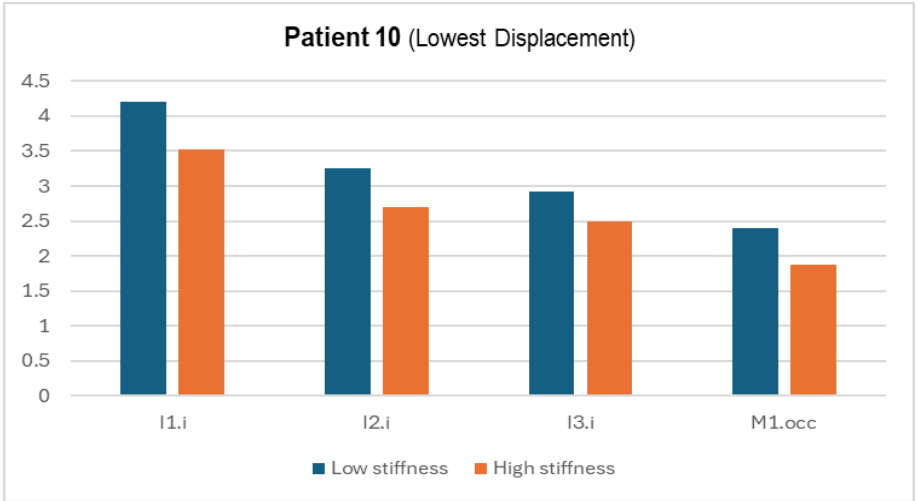

Figure 5.4: Lowest displacement (x10^3 mm) under thickness variation, found in one of the experimental models, subjected to variation in stiffness (high and lowest among all cadavers). Note the greater displacement under low stiffness.

CHAPTER 6

CONCLUSION

Stress distribution was highest at the canine, followed by the lateral incisor and central incisor. Relative to displacement, the central incisor exhibited lower stress and more displacement compared to the lateral incisor and canine. In contrast, the lateral incisor and canine showed higher stress accumulation with relatively lower displacement, indicating increased resistance to movement. These differences may be attributed to anatomical factors (e.g. tooth location within the arch and corresponding compact bone, root length and area of the canine).

The results demonstrate that anchorage modality significantly influences both stress distribution and displacement patterns. The buccal anchorage modality resulted in the highest displacement values across the studied teeth, followed by the bucco-palatal and palatal modalities. The palatal modality resulted in canine tipping, as the apex moved in slightly opposite direction of the crown. This tipping would require control or compensatory correction clinically.

300 g of force resulted in significantly greater displacement of the studied maxillary teeth with subsequent higher stress levels recorded at the level of the PDL.

The strength of the model in comparison with most FEA study related to the inclusion of individual variation of mechanical properties. The findings demonstrate that stiffness defines resistance to displacement more than thickness, further corroborating earlier results.

Further studies should explore the long-term effects of stress distribution on alveolar bone remodeling, based on separate CT scans of multiple individuals rather than

modifying the properties of a single model to simulate anatomical variations, and incorporating time-dependent simulations to model continuous tooth movement. Ultimately, clinical validation through patient-specific finite element modeling will enhance the applicability of these findings.

REFERENCES

Achmad, H., & Sesioria, A. (2022). Effects of Bionator Devices on Orofacial Muscle Strength in the Treatment of Class II Malocclusion in Developmental Phase: Systematic Review. *European Journal of Dental and Oral Health, 3*, 21-27.

Agrawal, R., Narang, S., Ahmed, H., Prasad, S., Reddy, S., & Aila, S. (2021). Influence of Occlusal Bite Forces on Teeth with Altered Periodontal Support: A Three-Dimensional Finite Element Stress Analysis. *Journal of Pharmacy and Bioallied Sciences, 13*(5), 688.

Alhasyimi, A. A., & Syahfik, I. (2023). Growth modification of developing Class II Division 1 malocclusion using myofunctional appliances. *Case Reports in Dentistry*.

Alemayehu, D. B., & Jeng, Y. R. (2021). Three-Dimensional Finite Element Investigation into Effects of Implant Thread Design and Loading Rate on Stress Distribution in Dental Implants and Anisotropic Bone. *Materials (Basel, Switzerland), 14*(22), 6974.

Alogaibi, Y. A., Al-Fraidi, A. A., Alhajrasi, M. K., Alkhathami, S. S., Hatrom, A., Afify, A. R., & Alhassan, M. A. (2021). Distalization in orthodontics: A review and case series. *Case Reports in Dentistry*, 2021, Article ID 8843959.

Ammar, H. H., Ngan, P., Crout, R. J., Mucino, V. H., & Mukdadi, O. M. (2011). Three-dimensional modeling and finite element analysis in treatment planning for orthodontic tooth movement. *American Journal of Orthodontics and Dentofacial Orthopedics, 139*(1), e59-71.

Ammoury, M. (2017). Effect of cortical bone quality and quantity on two orthodontic distalization modalities: a finite element analysis study.

Ammoury, M. J., Mustapha, S., Dechow, P. C., & Ghafari, J. G. (2019). Two distalization methods compared in a novel patient-specific finite element analysis. *American Journal of Orthodontics and Dentofacial Orthopedics, 156*(3), 326–336.

Ammoury, M. J., Mustapha, S., Dechow, P. C., & Ghafari, J. G. (2019). Two distalization methods compared in a novel patient-specific finite element analysis. *American Journal of Orthodontics and Dentofacial Orthopedics*, 326-336.

Andreasen, G. F., & Zwanziger, D. (1980). A clinical evaluation of the differential force concept as applied to the edgewise bracket. *American Journal of Orthodontics, 78*(1), 25–40.

Arat, M. K., Köklü, A., Özdiler, E., Rübendüz, M., & Erdoğan, B. (2001). Craniofacial growth and skeletal maturation: A mixed longitudinal study. *European Journal of Orthodontics, 23*(4), 355–361.

Arcuri, C., Muzzi, F., Santini, F., Barlattani, A., & Giancotti, A. (2007). Five years of experience using palatal mini-implants for orthodontic anchorage. *Journal of Oral and Maxillofacial Surgery, 65*(12), 2492–2497.

Ashcroft, I. M., Mubashar, A., Critchlow, G. W., & Crocombe, A. D. (2017). Moisture absorption–desorption effects in adhesive joints. In H. S. Nalwa (Ed.), *Handbook of Adhesion Technology* (pp. 199–226).

Aftabi, H., Zaraska, K., Eghbal, A., McGregor, S., Prisman, E., Hodgson, A., & Fels, S. (2024). Computational models and their applications in biomechanical analysis of mandibular reconstruction surgery. *Computers in Biology and Medicine, 169*, 107887.

Bayome, M. P., Park, J. H., Bay, C., & Kook, Y. A. (2021). Distalization of maxillary molars using temporary skeletal anchorage devices: A systematic review and meta-analysis. *Orthodontics & Craniofacial Research, 24*(Suppl 1), 103–112.

Bechtold, T. E., Kim, J.-W., Choi, T.-H., Park, Y.-C., & Lee, K.-J. (2013). Distalization pattern of the maxillary arch depending on the number of orthodontic miniscrews. *The Angle Orthodontist, 83*(2), 266–273..

Benca, E. A., Sasiadek, M., Mikołajczak, M., & Kwiatkowski, K. (2020). Effect of CT imaging on the accuracy of finite element modeling in bone. *European Radiology Experimental, 4*, Article number: 51.

Beyling, F. K., Klang, E., Niehoff, E., Wiechmann, D., & Janssens, Y. (2021). Class II correction by maxillary en masse distalization using a completely customized lingual appliance and a novel mini-screw anchorage concept: Preliminary results. *Head & Face Medicine, 17*, Article number: 23.

Bhai, K. J., Judge, R., Abduo, J., & Palamara, J. (2021). Measuring tooth movement with treatment using the Dahl principle: An observational study. *The Journal of Prosthetic Dentistry*. Advance online publication.

Boțilă, M.-R., Popa, D. L., Mercuț, R., Iacov-Crăițoiu, M. M., Scrieciu, M., Popescu, S. M., & Mercuț, V. (2024). A finite element method study of stress distribution in dental hard tissues: Impact of access cavity design and restoration material. *Bioengineering, 11*(9), 878.

Burstone, C. J., & Smith, J. R. (1984). Mechanics of tooth movement. *American Journal of Orthodontics, 85*(4), 294-307.

Buschang, P. H. (2014). Class I malocclusions—The development and etiology of mandibular malalignments. *Seminars in Orthodontics, 20*(1), 3–15

Bourassa, C., Hosein, Y. K., Pollmann, S. I., Galil, K., Bohay, R. N., Holdsworth, D. W., & Tassi, A. (2018). In-vitro comparison of different palatal sites for orthodontic miniscrew insertion: Effect of bone quality and quantity on primary stability. *American Journal of Orthodontics and Dentofacial Orthopedics, 154*(6), 809–819.

Ceratti, C., Serafin, M., Del Fabbro, M., & Caprioglio, A. (2024). Effectiveness of miniscrew-supported maxillary molar distalization according to temporary anchorage device features and appliance design: systematic review and meta-analysis. *The angle orthodontist*, 94(1): 107-121.

Chugh, T., Ganeshkar, S. V., Revankar, A. V., & Jain, A. K. (2013). Quantitative assessment of interradicular bone density in the maxilla and mandible: implications in clinical orthodontics. *Progress in Orthodontics, 14*(1):38.

Ciarlantini, R., & Melsen, B. (2012). Miniscrew-retained pontics in growing patients: a biological approach. *Journal of Clinical Orthodontics: JCO, 46*(10), 638–632.

Cerritelli, L., Hatzopoulos, S., Catalano, A., Bianchini, C., Cammaroto, G., Meccariello, G., Iannella, G., Vicini, C., Pelucchi, S., Skarzynski, P. H., & Ciorba, A. (2022). Rapid maxillary expansion (RME): An otolaryngologic perspective. *Journal of Clinical Medicine, 11*(17), 5243.

Cervinara, F. C., Cianci, C., De Cillis, F., Pappalettera, G., Pappalettere, C., Siciliani, G., & D'Apuzzo, F. (2019). Experimental study of the pressures and points of application of the forces exerted between aligner and tooth. *Nanomaterials, 9*(7), 1010.

Chang, Y., Tambe, A. A., Maeda, Y., Wada, M., & Gonda, T. (2018). Finite element analysis of dental implants with validation: To what extent can we expect the model to predict biological phenomena? A literature review and proposal for classification of a validation process. *International Journal of Implant Dentistry, 4*(1), 7.

Chen, G. T., Teng, F., & Xu, T.-M. (2016). Distalization of the maxillary and mandibular dentitions with miniscrew anchorage in a patient with moderate Class I bimaxillary dentoalveolar protrusion. *American Journal of Orthodontics and Dentofacial Orthopedics, 149*(3), 401–410.

Choi, Y. J., Lee, J.-S., Cha, J.-Y., & Park, Y.-C. (2011). Total distalization of the maxillary arch in a patient with skeletal Class II malocclusion. *American Journal of Orthodontics and Dentofacial Orthopedics, 139*(6), 823–833.

Cicciù, M. (2020). Bioengineering methods of analysis and medical devices: A current trends and state of the art. *Materials, 13*(3), 797.

Consolaro, A. (2014). Force distribution is more important than its intensity! *Dental Press Journal of Orthodontics, 19*(1), 5-7.

Crismani, A. G., Bertl, M. H., Celar, A. G., Bantleon, H.-P., & Burstone, C. J. (2010). Miniscrews in orthodontic treatment: Review and analysis of published clinical trials. *American Journal of Orthodontics and Dentofacial Orthopedics, 137*(1), 108–113.

Cowin, S. C., & Hart, R. T (1990). Errors in the orientation of the principal stress axes if bone tissue is modeled as isotropic. *Journal of Biomechanics, 23*(4), 349-352.

Dastgerdi, A. K., Yahyaiee Bavil, A., & Rouhi, G. (2023). The effects of material and structural properties of the periodontal ligament in mechanical function of tooth-PDL-bone complex in dental trauma: A sensitivity study using finite element analysis. *Proceedings of the Institution of Mechanical Engineers, Part H: Journal of Engineering in Medicine*, 237(5), 619–627.

Elkordy, S. A., Abouelezz, A. M., Fayed, M. M. S., Aboulfotouh, M. H., & Mostafa, Y. A. (2019). Evaluation of the miniplate-anchored Forsus Fatigue Resistant Device in skeletal Class II growing subjects: *A randomized controlled trial*. *The Angle orthodontist*, *89*(3), 391–403.

Enzo, B. (2020). Malocclusion in orthodontics and oral health: Adopted by the General Assembly: September 2019, San Francisco, United States of America. *International Dental Journal*, 70(1), 11–12.

Fabra Rivera, A. M., Magalhães, F. de C., Moreno, A., & Campos Rubio, J. (2020). Assessment of the highest stress concentration area generated on the mandibular structure using meshless finite elements analysis. *Bioengineering, 7*(4), 142.

Falcinelli, C., Valente, F., Vasta, M., & Traini, T. (2023). Finite element analysis in implant dentistry: State of the art and future directions. *Dental Materials, 39*(6), 539–556.

Feng, Y., Kong, W. D., Cen, W. J., Zhou, X. Z., Zhang, W., Li, Q. T., Guo, H. Y., & Yu, J. W. (2019). Finite element analysis of the effect of power arm locations on tooth movement in extraction space closure with miniscrew anchorage in customized lingual orthodontic treatment. *American Journal of Orthodontics and Dentofacial Orthopedics, 156*(2), 210-219.

Fill, T. S., Toogood, R. W., Major, P. W., & Carey, J. P. (2012). Analytically determined mechanical properties of, and models for the periodontal ligament: critical review of literature. *Journal of Biomechanics, 45*(1), 9-16.

Fujita, Y., Kimura, H., & Yanagisawa, W. (2014). Experimental verification of finite element analysis for a thermoplastic orthodontic aligner. *The Showa University Journal of Medical Sciences, 26*(2), 139–147.

Geng, J. P., Tan, K. B., & Liu, G. R. (2001). Application of finite element analysis in implant dentistry: a review of the literature. *The Journal of Prosthetic Dentistry, 85*(6), 585–598.

Ghafari, J. G., Shofer, F. S., Jacobsson-Hunt, U., Markowitz, D. L., & Laster, L. L. (1998). Headgear versus function regulator in the early treatment of Class II, Division 1 malocclusion: A randomized clinical trial. *American Journal of Orthodontics and Dentofacial Orthopedics, 113*(1), 51–61.

Ghafari, J. G., Ziade, E. G., Kassab, A., Saadeh, M., & Macari, A. T. (2025). Variation of chin morphology and mandibular incisor length in different facial divergence patterns: New insights from CBCT records. *Orthodontics & Craniofacial Research, 28*(1), 142–150.

Ghodasra, R., & McReynolds, B. (2024). Orthodontics, malocclusion. [Updated 2023 Apr 23]. In *StatPearls* [Internet]. StatPearls Publishing.

Gurgel, M. L.-B., Silva, D. M., Lima, D. S., & Oliveira, D. D. (2023). Clear aligner mandibular advancement in growing patients with Class II malocclusion. *AJO-DO Clinical Companion, 3*(2), 93–109.

Hedayati, Z., & Shomali, M. (2016). Maxillary anterior en masse retraction using different antero-posterior position of mini screw: a 3D finite element study. *Progress in orthodontics*, 17(1), 31.

Henneman, S. V., Forriol, F., & Ngan, P. (2008). Mechanobiology of tooth movement. *European Journal of Orthodontics*, 30(3), 299–306.

Jamachi, C., & Beatriz, V. (2019). Finite element analysis in orthodontics. *Journal of Orthodontics and Facial Orthopedics*, 29(2), 150–159.

Jheon, A. H., O'Higgins, P., & Jones, S. (2013). From molecules to mastication: The development and evolution of teeth. *Wiley Interdisciplinary Reviews: Developmental Biology*, 32(2), 165–182.

Jiang, F. R., Li, Y., Zhang, C., & Xu, Z. (2020). Mechanical environment for lower canine T-loop retraction compared to en-masse space closure with a power-arm attached to either the canine bracket or the archwire. *The Angle Orthodontist*, 90(6), 801–810.

Kalia, H., Gupta, S., Ahuja, S., Bhambri, E., Goyal, A., & Sharma, R. (2019). Evaluation of stress pattern in periodontium and change in inclination during en masse retraction: Finite element analysis. *Journal of the World Federation of Orthodontists*, 153–158.

Kang, J. M., Choi, Y. J., Kim, Y. H., & Lee, K. J. (2016). A three-dimensional finite element analysis of molar distalization with a palatal plate, pendulum, and headgear according to molar eruption stage. *Korean Journal of Orthodontics, 46*(5), 290–300.

Karvelas, N., Dragomir, B. R., Chehab, A., Panaite, T., Papadopoulos, M. A., & Zetu, I. (2023). Non-compliance distalization appliances supported by mini-implants: A systematic review. *Applied Sciences, 13*(8), 5176.

Kawamura, J., Park, J. H., Kojima, Y., Tamaya, N., Kook, Y. A., Kyung, H. M., & Chae, J. M. (2021). Biomechanical analysis for total distalization of the maxillary dentition: A finite element study. *American Journal of Orthodontics and Dentofacial Orthopedics, 160*(2), 259–265.

Kawamura, J., Park, J. H., Kojima, Y., Tamaya, N., Kook, Y. A., Kyung, H. M., & Chae, J. M. (2021). Biomechanical analysis for total mesialization of the maxillary dentition: A finite element study. *American Journal of Orthodontics and Dentofacial Orthopedics, 159*(6), 790–798.

Khan, J., Goyal, M., Kumar, M., Kushwah, A., Kaur, A., & Sharma, M. (2021). Comparative evaluation of displacement and stress distribution pattern during maxillary arch distalization with Infra Zygomatic Screw—A three-dimensional finite element study. *International Orthodontics*, 291–300.

Kim, H. S., Kim, Y. H., Park, J. K., & Lee, J. Y. (2012). Finite element modeling technique for predicting mechanical behaviors on mandible bone during mastication. *The Journal of Advanced Prosthodontics, 4*(4), 218–226.

Kinzinger, G. S. (2007). Efficiency of a skeletonized distal jet appliance supported by miniscrew anchorage for noncompliance maxillary molar distalization. *American Journal of Orthodontics and Dentofacial Orthopedics, 136*(4), 578–586.

Kinzinger, G. S., Diedrich, P. R., & Bowman, S. J. (2006). Upper molar distalization with a miniscrew-supported Distal Jet. *Journal of Clinical Orthodontics: JCO, 40*(11), 672–678.

Knop, L. G., Santos, F. A., & Lopes, P. A. (2015). Scientific use of the finite element method in orthodontics. *Dental Press Journal of Orthodontics, 20*(2), 119–125.

Kuc, A. E., Górska, J., & Kuc, D. (2024). The hydrostatic pressure distribution in the periodontal ligament and the risk of root resorption: A finite element method (FEM) study on the nonlinear innovative model. *Materials (Basel, Switzerland), 17*(7), 1661.

Oliviero, L. S. (2022). Improving headgear wear: Why force level and direction of traction matter. *European Journal of Orthodontics*, 44(2), 174–179.

Lee, S. K., Abbas, N. H., Bayome, M., Baik, U. B., Kook, Y. A., Hong, M., & Park, J. H. (2018). A comparison of treatment effects of total arch distalization using modified C-palatal plate vs buccal miniscrews. *The Angle Orthodontist, 88*(1), 45–51.

Lindh, C., Obrant, K., & Petersson, A. (2004). Maxillary bone mineral density and its relationship to the bone mineral density of the lumbar spine and hip. *Oral Surgery, Oral Medicine, Oral Pathology, Oral Radiology, Endodontics, 98*(1), 102–109.

Li, Y. Z., Zhang, X., Zhang, X. M., & He, H. (2021). Biomechanical and biological responses of periodontium in orthodontic tooth movement: Update in a new decade. *International Journal of Oral Science, 13*(1), 20.

Lisiak-Myszke, M. M., Czerwinski, F., Siennicka, A., & Chmielnicki, M. (2020). Application of finite element analysis in oral and maxillofacial surgery: A literature review. *Materials (Basel, Switzerland), 13*(14), 3063.

Liu, C., Zhu, X., & Zhang, X. (2015). Three-dimensional finite element analysis of maxillary protraction with labiolingual arches and implants. *American Journal of Orthodontics and Dentofacial Orthopedics, 148*(3), 466–478.

Matos, J. D., Ferreira, P., Souza, J., & Oliveira, A. (2022). Bioengineering tools applied to dentistry: Validation methods for in vitro and in silico analysis. *Dentistry Journal, 10*(8), 145.

Melsen, B. M., Huja, S. S., Chien, H. H. B., & Dalstra, M. (2014). Alveolar bone preservation subsequent to miniscrew implant placement in a canine model. *Orthodontics & Craniofacial Research, 18*(2), 77–85.

Middleton, J., Jones, M., & Wilson, A. (1996). The role of the periodontal ligament in bone modeling: The initial development of a time-dependent finite element model. *American Journal of Orthodontics and Dentofacial Orthopedics, 109*(2), 155–162.

Moga, R. A., Săftoiu, A., Popa, D., & al. (2023). Assessment of the maximum amount of orthodontic force for PDL in intact and reduced periodontium (Part I). *International Journal of Environmental Research and Public Health, 20*(3), 1889.

Mohamed, R. N., Basha, S., & Al-Thomali, Y. (2018). Maxillary molar distalization with miniscrew-supported appliances in Class II malocclusion: A systematic review. *The Angle Orthodontist, 88*(4), 494–502.

Noorollahian, S., Alavi, S., & Shirban, F. (2016). Bilateral en-masse distalization of maxillary posterior teeth with skeletal anchorage: a case report. *Dental press journal of orthodontics*, *21*(3), 85–93.

Papadopoulos, M. A., & Tarawneh, F. (2007). The use of miniscrew implants for temporary skeletal anchorage in orthodontics: A comprehensive review. *Oral Surgery, Oral Medicine, Oral Pathology, Oral Radiology, and Endodontics, 103*(5), e6–e15.

Park, C. O., Sa'aed, N. L., Bayome, M., Park, J. H., Kook, Y. A., Park, Y. S., & Han, S. H. (2017). Comparison of treatment effects between the modified C-palatal plate

and cervical pull headgear for total arch distalization in adults. *Korean Journal of Orthodontics, 47*(6), 375–383.

Park, J. H., Saito, T., Yoo, S. K., Alfaifi, M., & Kook, Y. A. (2020). Distalization with a modified C-palatal plate for severe upper crowding and a missing lower incisor. *Korean Journal of Orthodontics, 50*(1), 52–62.

Pellegrino, G., Lizio, G., Ferri, A., & Marchetti, C. (2021). Flapless and bone-preserving extraction of partially impacted mandibular third molars with dynamic navigation technology: A report of three cases. *International Journal of Computerized Dentistry, 24*(3), 253–262.

Peterson, J., Wang, Q., & Dechow, P. C. (2006). Material properties of the dentate maxilla. *The Anatomical Record Part A: Discoveries in Molecular, Cellular, and Evolutionary Biology,* 933–1030.

Phellan, R., Hachem, B., Clin, J., Mac-Thiong, J.-M., & Duong, L. (2020). Real-time biomechanics using the finite element method and machine learning: Review and perspective. *Medical Physics, 48*(1), 7–18.

Prasad, S. E., Sudhakar, R., Arul, R. G., & Kumar, P. M. (2014). Pathognomonic features of Angle's Class II division 2 malocclusion: A comparative cephalometric and arch width study. *Journal of International Society of Preventive & Community Dentistry, 4*(Suppl 2), S105–S109.

Proffit, W. R., Fields, H. W., Jr, & Moray, L. J. (1998). Prevalence of malocclusion and orthodontic treatment need in the United States: estimates from the NHANES III survey. *The International journal of adult orthodontics and orthognathic surgery*, *13*(2), 97–106.

Raghis, T., Alfrih Alsulaiman, T. M., Mahmoud, G., & Youssef, M. (2022). Efficiency of maxillary total arch distalization using temporary anchorage devices (TADs) for treatment of Class II malocclusions: A systematic review and meta-analysis. *International Orthodontics, 20*(3), 100666.

Reddy, M. S., Sundram, R., & Eid Abdemagyd, H. A. (2019). Application of finite element model in implant dentistry: A systematic review. *Journal of Pharmacy & Bioallied Sciences, 11*(Suppl 2), S85–S91.

Rédua, R. (2020). Different approaches to the treatment of skeletal Class II malocclusion during growth: Bionator versus extraoral appliance. *Dental Press Journal of Orthodontics, 25*(2), 69–85.

Riachy, P. (2023). Evaluation of different osteotomies in surgically assisted rapid palatal expansion: A finite element analysis study. *AUB Publication.*

Ritchie, C., McGregor, S., & Bearn, D. R. (2023). Temporary anchorage devices and the forces and effects on the dentition and surrounding structures during orthodontic treatment: A scoping review. *European Journal of Orthodontics, 45*(3), 324–337.

Rizwana, A., Gandhi, A., Rai, P., & Tripathi, T. (2024). Miniplate-anchored Forsus fatigue-resistant device with a fail-safe attachment. *AJO-DO Clinical Companion, 4*(6).

Roberts, W. E., Arbuckle, G. R., & Analoui, M. (1996). Rate of mesial translation of mandibular molars using implant-anchored mechanics. *The Angle Orthodontist, 66*(5), 331–338.

Roesch, Z. K., & Tadi, P. (2023, July 24). Anatomy, head and neck, neck. *StatPearls*

Satpathy, M., Duan, Y., Betts, L., Priddy, M., & Griggs, J. A. (2022). Effect of bone remodeling on dental implant fatigue limit predicted using 3D finite element analysis. *Journal of Dentistry and Oral Epidemiology, 2*(1), 10.54289/jdoe2200102.

Schwertner, A., de Almeida-Pedrin, R. R., Poleti, T. M. F. F., Oltramari, P., de Castro Conti, A. C. F., Cotrim-Ferreira, F. A., de Almeida, G., Flores-Mir, C., & de Almeida, M. R. (2024). Biomechanical analysis of total arch maxillary distalization using infrazygomatic crest miniscrews: A finite element analysis study. *Progress in Orthodontics, 25*(1), 10.

Shinya, K., Shinya, A., Nakahara, R., Nakasone, Y., & Shinya, A. (2009). Characteristics of the tooth in the initial movement: The influence of the restraint site to the periodontal ligament and the alveolar bone. *The Open Dentistry Journal, 3*, 85–91.

Singh, D. P., Arora, S., Yadav, S. K., & Kedia, N. B. (2017). Intraoral approaches for maxillary molar distalization: Case series. *Journal of Clinical and Diagnostic Research: JCDR, 11*(5), ZR01–ZR04.

Singh, J. R., Kambalyal, P., Jain, M., & Khandelwal, P. (2016). Revolution in orthodontics: Finite element analysis. *Journal of International Society of Preventive & Community Dentistry, 6*(2), 110–114.

Song, J. W., Lim, J. K., Lee, K. J., Sung, S. J., Chun, Y. S., & Mo, S. S. (2016). Finite element analysis of maxillary incisor displacement during en-masse retraction according to orthodontic mini-implant position. *The Korean Journal of Orthodontics*, 242–252.

Stalpers, M. J., Booij, J. W., Bronkhorst, E. M., Kuijpers-Jagtman, A. M., & Katsaros, C. (2007). Extraction of maxillary first permanent molars in patients with Class II Division 1 malocclusion. *American Journal of Orthodontics and Dentofacial Orthopedics, 132*(3), 316–323.

Stephens, C. K., Boley, J. C., Behrents, R. G., Alexander, R. G., & Buschang, P. H. (2005). Long-term profile changes in extraction and nonextraction patients. *American Journal of Orthodontics and Dentofacial Orthopedics, 128*(4), 450–457.

Sugawara, J., Kanzaki, R., Takahashi, I., Nagasaka, H., & Nanda, R. (2006). Distal movement of maxillary molars in nongrowing patients with the skeletal anchorage system. *American Journal of Orthodontics and Dentofacial Orthopedics, 129*(6), 723–733.

Sujaritwanid, K., Suzuki, B., & Suzuki, E. Y. (2021). Comparison of one versus two maxillary molars distalization with iPanda: A finite element analysis. *Progress in Orthodontics, 22*(1), 12.

Sun, C., Zhou, Z., Shi, H., Algahefi, A., & Li, Z. (2025). Enhanced pendulum appliance utilizing temporary anchorage device-based Nance arch and modified springs for optimized molar distalization control: A case report. *The Angle Orthodontist, 95*(1), 126–136.

Sung, E. H., Kim, S. J., Chun, Y. S., Park, Y. C., Yu, H. S., & Lee, K. J. (2015). Distalization pattern of whole maxillary dentition according to force application points. *The Korean Journal of Orthodontics, 45*(1), 20–28.

Sung, S. J., Jang, G. W., Chun, Y. S., & Moon, Y. S. (2010). Effective en-masse retraction design with orthodontic mini-implant anchorage: A finite element analysis. *American Journal of Orthodontics and Dentofacial Orthopedics, 137*(5), 648–657.

Tadic, N., & Woods, M. G. (2007). Incisal and soft tissue effects of maxillary premolar extraction in class II treatment. *The Angle Orthodontist, 77*(5), 808–816.

Tanne, K., Sakuda, M., & Burstone, C. J. (1987). Three-dimensional finite element analysis for stress in the periodontal tissue by orthodontic forces. *American Journal of Orthodontics and Dentofacial Orthopedics, 92*(6), 499–505.

Theodorou, C. I., Kuijpers-Jagtman, A. M., Bronkhorst, E. M., & Wagener, F. A. D. T. G. (2019). Optimal force magnitude for bodily orthodontic tooth movement with fixed appliances: A systematic review. *American Journal of Orthodontics and Dentofacial Orthopedics, 156*(5), 582–592.

Tian, T., Huang, H. Y., Wang, W., Shi, B., Zheng, Q., & Li, C. H. (2022). Three-dimensional finite element analysis of the effect of alveolar cleft bone graft on the maxillofacial biomechanical stabilities of unilateral complete cleft lip and palate. *Biomedical Engineering Online, 21*(1), 31.

Trivedi, S. (2014). Finite element analysis: A boon to dentistry. *Journal of Oral Biology and Craniofacial Research, 4*(3), 200–203.

Truong, V. M., Kim, S., Kim, J., Lee, J. W., & Park, Y. S. (2022). Revisiting the complications of orthodontic miniscrew. *BioMed Research International, 2022*, 8720412.

Uhlir, R., Mayo, V., Lin, P. H., Chen, S., Lee, Y. T., Hershey, G., Lin, F. C., & Ko, C. C. (2017). Biomechanical characterization of the periodontal ligament: Orthodontic tooth movement. *The Angle orthodontist*, *87*(2), 183–192.

Whyte, A., & Boeddinghaus, R. (2019). The maxillary sinus: physiology, development and imaging anatomy. *Dento maxillo facial radiology*, *48*(8), 20190205.

Wilmes, B., & Drescher, D. (2010). Application and effectiveness of the Beneslider: a device to move molars distally. *World journal of orthodontics*, *11*(4), 331–340.

Yelick, P. C., & Sharpe, P. T. (2019). Tooth Bioengineering and Regenerative Dentistry. *Journal of dental research*, *98*(11), 1173–1182.

Yu, I. J., Kook, Y. A., Sung, S. J., Lee, K. J., Chun, Y. S., & Mo, S. S. (2014). Comparison of tooth displacement between buccal mini-implants and palatal plate anchorage for molar distalization: a finite element study. *European journal of orthodontics*, *36*(4), 394–402.

Zeno, K. G. (2017). *Orthodontic traction of palatally impacted canines: A finite element analysis study* (Master's thesis). American University of Beirut.

Zeno, K. G., & Ammoury, M. J. (2023). The surge of finite element analysis in the study of orthodontic mechanics: Are the findings applicable in practice? *Seminars in Orthodontics, 29*(4), 308–316.

Zeno, K. G., Mustapha, S., Ayoub, G., & Ghafari, J. G. (2020). Effect of force direction and tooth angulation during traction of palatally impacted canines: A finite element analysis. *American Journal of Orthodontics and Dentofacial Orthopedics, 157*(3), 377–384.

Zhang, W., Skrypczak, A., & Weltman, R. (2015). Anterior maxilla alveolar ridge dimension and morphology measurement by cone beam computerized tomography (CBCT) for immediate implant treatment planning. *BMC Oral Health, 15*, 65.